DEPARTMENT OF NATIONAL RESOURCES

BUREAU OF MINERAL RESOURCES, GEOLOGY AND GEOPHYSICS

Record 1977/9

RUM JUNGLE AREA GRAVITY SURVEY NORTHERN TERRITORY 1974

by

J.A. MAJOR

Record 1977/9

RUM JUNGLE AREA GRAVITY SURVEY
NORTHERN TERRITORY
1974

by
J.A. MAJOR

CONTENTS

TABLES

FIGURES

PLATES

SUMMARY

Between May and September 1974 the Bureau of Mineral Resources made a gravity survey on and around the Rum Jungle and Waterhouse Complexes. The survey had as objectives the investigation of the relations between the basement complexes and the metasediments and the delineation of the Coomalie Dolomite/Golden Dyke Formation boundary. To achieve these objectives, 744 km of regional traverses with a 500-m station spacing were read on and around the complexes, and 26 km of detailed traverses with a 40-m station spacing were read across the Coomalie Dolomite/Golden Dyke Formation boundary.

The gravity method cannot be used to map the complex/sediment contact everywhere. This is because parts of the complexes have the same density as the surrounding metasediments. However, in most areas there is a density contrast between the complexes and the metasediments and in these areas the geometry of the low-density parts of the complexes can be determined. Two-dimensional models, corrected for end effects, suggest that the metasediments extend no deeper than four kilometres. Calculations of deficient mass support this depth estimate.

The sediments in the embayment deepen to the west and contain dense material which is probably amphibolite or massive dolomite.

The gravity method is not suitable for detecting the Coomalie Dolomite/Golden Dyke Formation boundary because there is no consistent density contrast across this boundary.

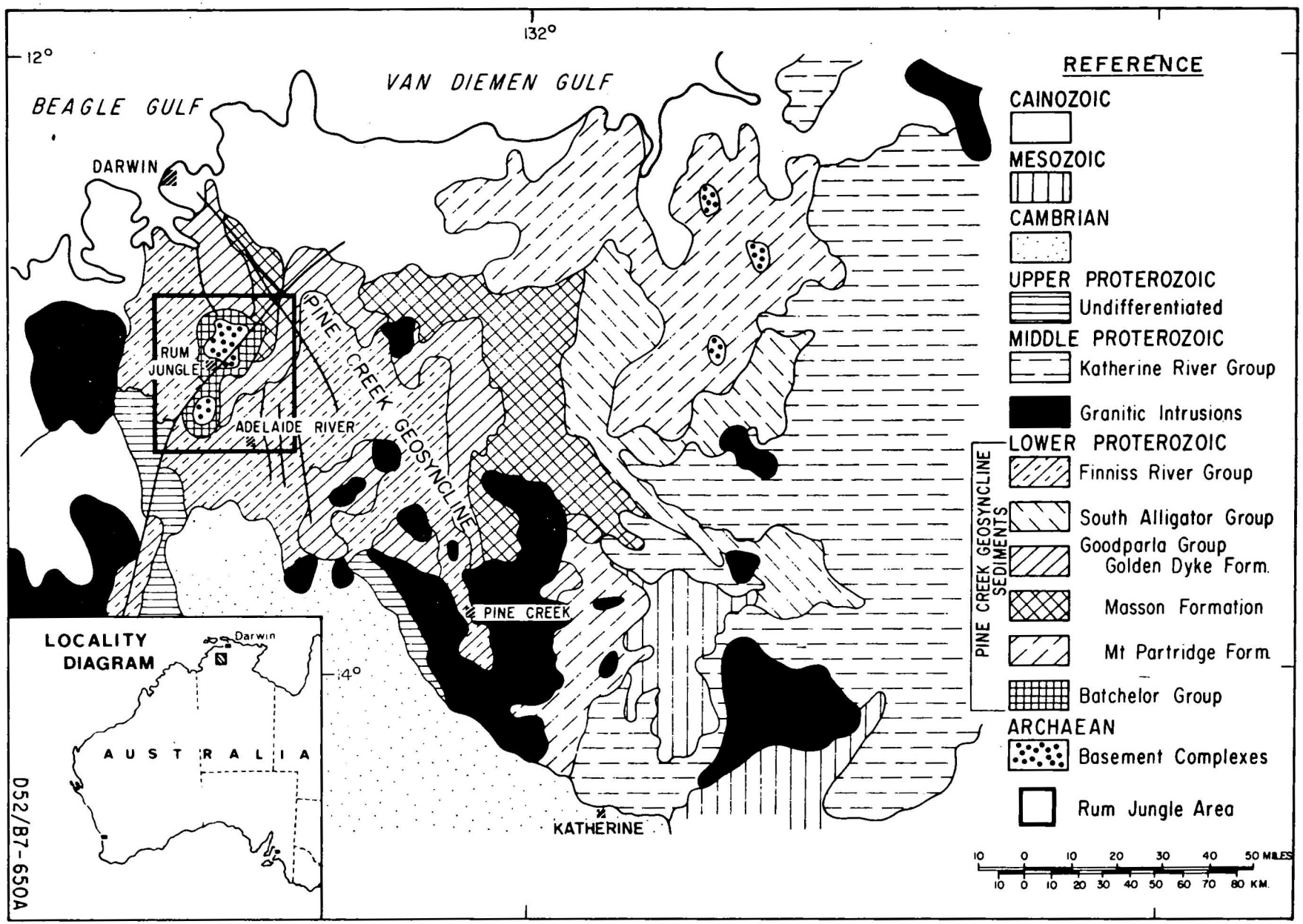

LOCALITY MAP AND GENERALIZED GEOLOGY OF THE KATHERINE-DARWIN AREA (After Walpole & Crohn, 1965 and Stephansson & Johnson, 1975)

Fig 1

1. INTRODUCTION

In the period 13 May to 19 September 1974 the Bureau of Mineral Resources (BMR) made a gravity survey in the Rum Jungle area of the Northern Territory. The area covered by the survey is bounded by latitudes 12° 45'S and 13° 17'S and longitudes 130° 51'E and 131° 12'E. The location and geological setting of the survey area are indicated in Figure 1.

The survey was carried out to investigate relations between the two basement complexes in the area and the surrounding metasediments, and to delineate the boundary between the Coomalie Dolomite and the Golden Dyke Formation. This boundary is of interest because the main uranium and base-metal deposits in the Rum Jungle area occur in the Golden Dyke Formation near its contact with the Coomalie Dolomite.

During the survey 26 km of detailed gravity traverses employing a 40-m station spacing were made across the Coomalie Dolomite/Golden Dyke Formation boundary and 744 km of regional traverses employing a 500-m station spacing were made across the Rum Jungle basement complexes.

In 1972-74 BMR remapped the Rum Jungle area (Johnson, 1974). This work included drilling a number of holes in 1973 and 1974. Physical property measurements were made on core from these holes, and the densities determined have been used in the interpretation of the gravity data.

2. GEOLOGY

The geology of the Pine Creek Geosyncline has been described by Walpole et al. (1968), and Figure 1 shows a generalised geological map of the geosyncline. Plate 1 is Johnson's (1974) solid geology map of the Rum Jungle area and shows the rock types in the area covered by the gravity survey.

Rhodes (1965) described the geology of the Rum Jungle Complex and its relation to the metasediments, Walpole et al. (1968) described the metasediments, and Johnson (1974) described the revised geology of the Rum Jungle area.

2.1 Basement complexes

The Rum Jungle Complex is a granitic complex which occupies the core of an eroded dome of low-grade metasediments of the Batchelor Group. Six major units have been distinguished in the Complex by Rhodes (1965); these are, in order of decreasing age: schists and gneisses, granite gneiss, metadiorite, coarse granite, large feldspar granite, and leucocratic granite. Rhodes's subdivisions are shown in Figure 2. Veins and dykes of pegmatite and amphibolite, and quartz-tourmaline veins, are also present. The metasediments rest unconformably on the eroded surface of the older granitic complexes. During a later period of folding and low-grade metamorphism the metasediments were domed around the granitic basement (Rhodes, 1965). At least part of the Rum Jungle Complex appears to be Archaean (Johnson, 1974).

The Waterhouse Complex is a complex of fine and coarse-grained granite and schist. The metasediments rest unconformably on the Complex (Johnson, 1974).

2.2 Lower Proterozoic sediments

Batchelor Group. Within the Batchelor Group only the Coomalie Dolomite will be discussed in detail since one of the objects of the 1974 survey work was to locate the boundary between the Coomalie Dolomite and the overlying Golden Dyke Formation.

Table 1 shows the stratigraphic successions around the eastern margins of the complexes and gives the estimated thicknesses and brief descriptions of the formations. For further details see Walpole et al., (1968) and Johnson (1974).

The Batchelor Group consists of the Beestons Formation, Celia Dolomite, Crater Formation, and Coomalie Dolomite. These comprise alternating clastic and chemical sediments. A littoral and neritic environment of deposition is indicated by:

(a) Algal reef masses found in both the Coomalie and Celia Dolomites;

(b) Variability of sediments within the Beestons and Crater Formations (see Table 1). This variability reflects the proximity of the Rum Jungle and Waterhouse Complexes, which are the basement rocks from which the sediments were derived.

Fig. 2

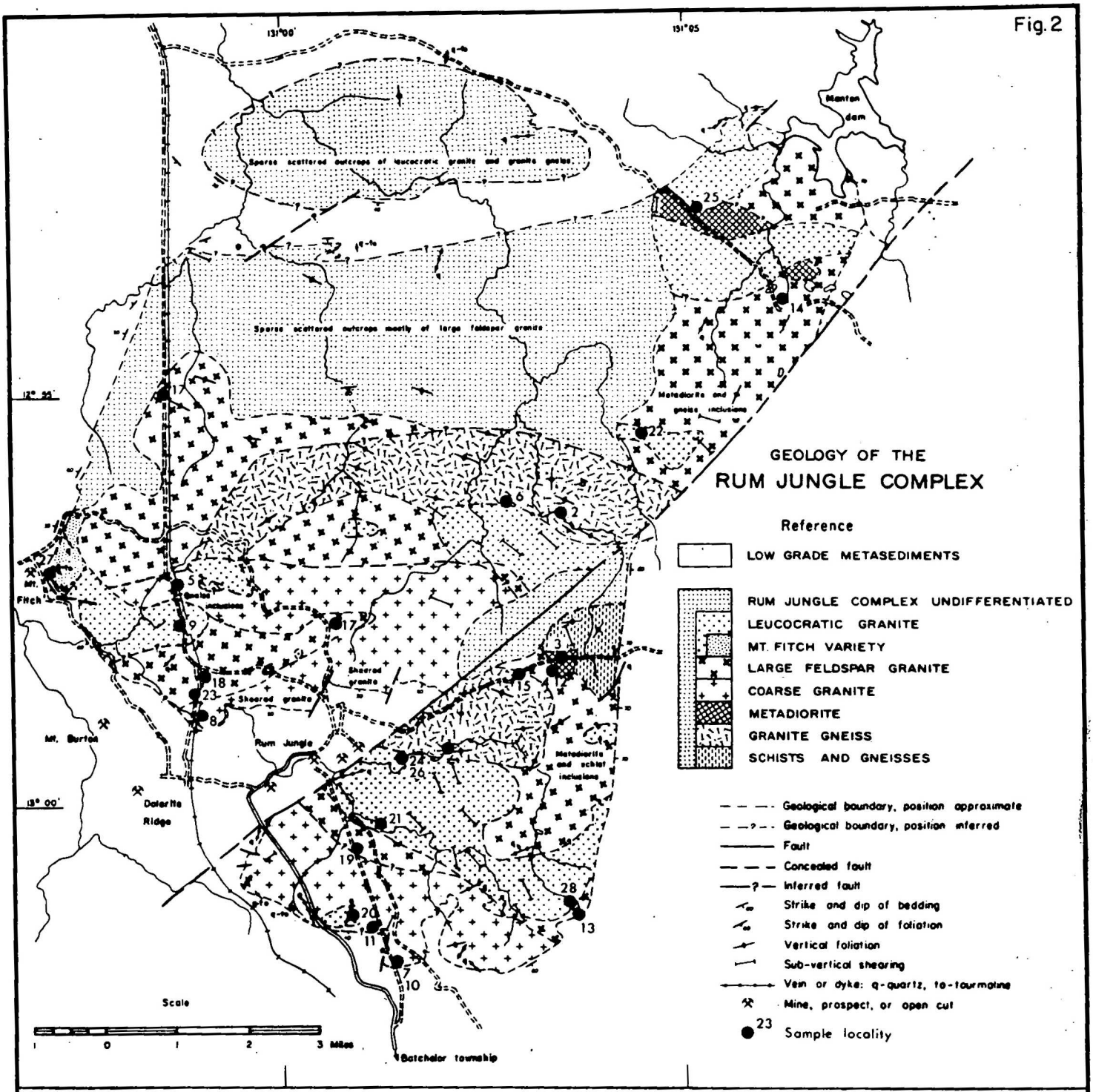

Record No. 1977/9
(Based on D52/A/7)

D52/B7-670A

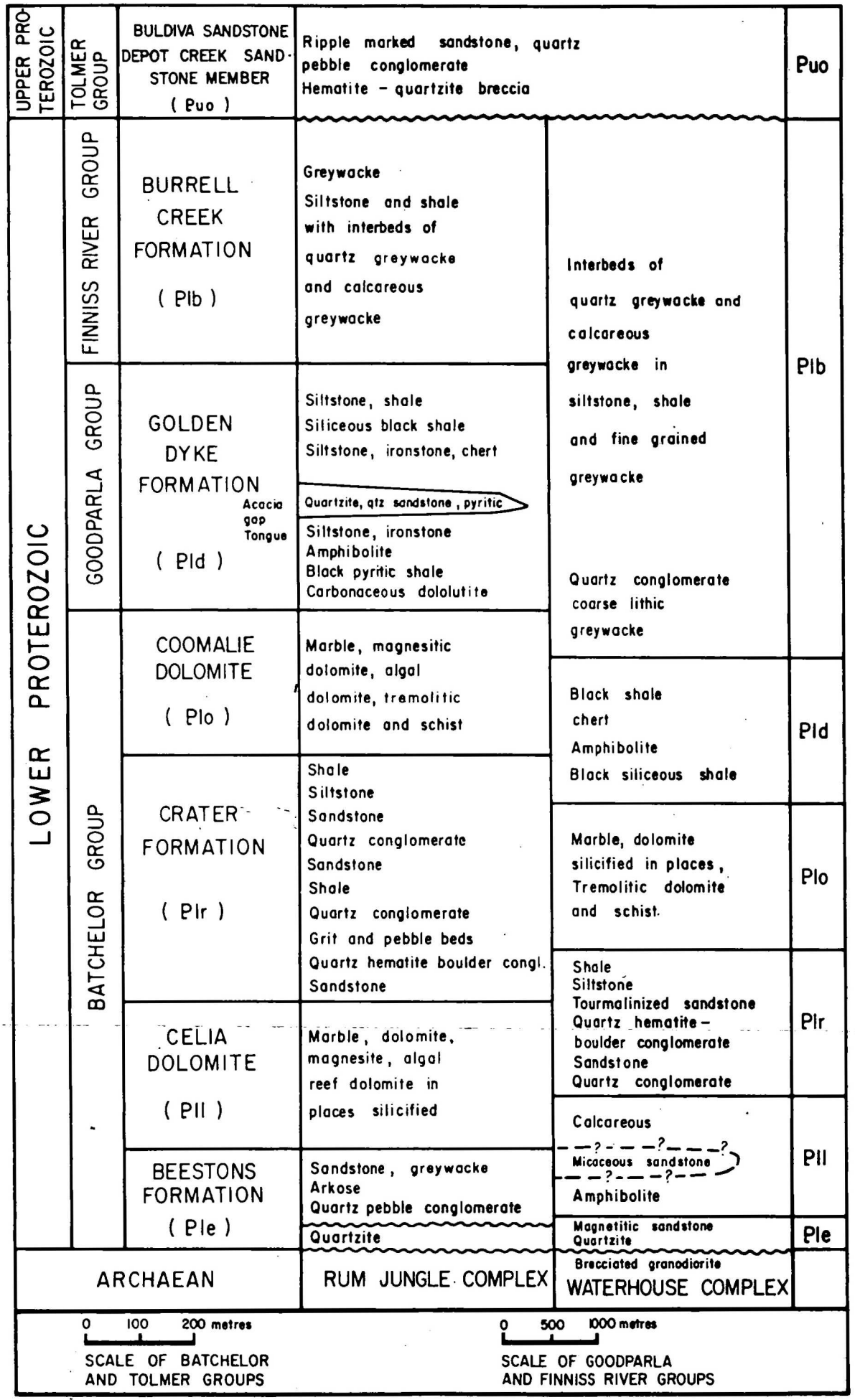

TABLE I. Stratigraphic successions around the eastern margins of the Rum Jungle and Waterhouse Complexes. D52/B7-671A

Record No. 1977/9

The Coomalie Dolomite is the youngest formation of the Batchelor Group and was deposited conformably on the Crater Formation. It was deposited under stable shallow-marine conditions and comprises algal dolomite, silicified dolomite, silicified dolomitic marl and slump breccia, tremolite schist, and coarse marble. In outcrop the Coomalie Dolomite is often heavily silicified or lateritised, or both. The Coomalie Dolomite marks the edge of the Batchelor shelf. The varying distance of the Coomalie Dolomite from the complexes indicates the asymmetry of this shelf, which was narrower on the western margins of the complexes, wider on the eastern margins, and widest between them.

Goodparla Group. The Goodparla Group is composed of sediments deposited in basins around or within the Batchelor shelf. The group consists of:

(a) The Golden Dyke Formation, a siltstone-mudstone sequence, composed of black shale, siltstone, quartzite, and ironstone.

(b) The Acacia Gap Tongue, a pyritic, massive quartzite, which is correlated with the Masson Formation further east.

Most of the uranium and base-metal deposits in the Rum Jungle area were found in the Golden Dyke Formation near the boundary with the underlying Coomalie Dolomite. On the eastern and southeastern boundary of the Rum Jungle Complex there is a transition zone between the Coomalie Dolomite and Golden Dyke Formation. This zone comprises black calcilutite and siltstone and grades up into strongly graphitic calcareous shale. The transition zone is part of the Golden Dyke Formation. East of the Waterhouse Complex the transition zone contains weakly pyritic calcareous pale green shale. In the Rum Jungle area the Golden Dyke Formation consists of carbonaceous siltstone, silicified dolomite and marl, and silicified dolomitic slump breccia. Pyrite is a common constituent of the carbonaceous rocks.

The Acacia Gap Tongue is a massive pyritic quartzite interbedded with shale of the Golden Dyke Formation and forms prominent ridges north, east, and west of the Rum Jungle Complex.

Finniss River Group. The Finniss River Group is divided into the Burrell Creek and Noltenius Formations and consists of flysch-type greywacke and siltstone deposited in troughs around the Batchelor shelf and Goodparla basin. It is developed only on the west of the Pine Creek Geosyncline and had a westerly provenance. The Noltenius Formation is predominantly greywacke, and the Burrell Creek Formation mainly siltstone. The formations grade into each other and the range of rock types reflects the closeness of the source area. The Noltenius Formation is coarser than the Burrell Creek Formation and was deposited closer to the source area.

2.3 Upper Proterozoic sediments

Tolmer Group: Depot Creek Sandstone Member. After the Finniss River Group was deposited, the Lower Proterozoic sediments were folded, faulted, and eroded. The Depot Creek Sandstone Member was deposited on an irregular erosion surface. The basal unit of thé member is a hematite-quartzite breccia (HQB), which is regarded as a regolith as it was formed over the Crater Formation, Coomalie Dolomite, and Golden Dyke, Noltenius, and Burrell Creek Formations.

2.4 Cainozoic

Most of the area is covered by superficial Cainozoic sand, laterite, black soil, and alluvium which are not significant in the gravity work.

2.5 Intrusives

Basic intrusives in the Golden Dyke Formation crop out at Dolerite Ridge and near Darwin River Siding. Buried amphibolites have been located by drilling. Most known amphibolites are in the Golden Dyke Formation, but in 1973 and 1974 auger drilling located amphibolite in the Coomalie and Celia Dolomites.

Some amphibolites are igneous while others are sedimentary. Bryan (1962) gives an example of a drill-hole at Rum Jungle Creek South which intersected 300 m of amphibolite comprising both types.

2.6 Structure

Williams (1963) believed the Rum Jungle area was subjected to four periods of folding which were responsible for the basement dome and basin structures. Rhodes (1965) supported Williams's idea that the sediments had not been intruded by the Rum Jungle Granite and that the doming of sediments around the complexes was produced by polyphase folding. Johnson (1974) discussed the relations between the Batchelor group and the basement complexes. He cited examples of granitisation and metasomatism which suggested that there had been both tectonism and thermal reactivation of the complexes resulting in doming of the basement and the overlying sediments.

Stephansson & Johnson (1975) believe there was diapiric intrusion of an Upper Proterozoic granite into the basement complexes. Structural evidence to support their idea is pebble deformation within steeply dipping beds of conglomerate, disappearance of polyphase fold rock structures away from the basement complexes, and bending of folded country rock strata into concordance with the complex/sediment contact. They suggest that there were two main tectonic events. These were:

(a) an east-west compression of the sediments in the whole geosyncline to produce folding along north-south axes. This folding is best seen in the shales of the Burrell Creek and Golden Dyke Formations;

(b) a later phase of deformation involving the doming of the two complexes.

According to Johnson (1974) the strike direction of the Finniss River and Goodparla Groups has been determined by the dominant fold direction, but the strike of the Batchelor Group reflects the original depositional strike, parallel to the margins of the basement complexes.

The Giants Reef Fault is the main structural feature of the area and was active from late Proterozoic to early Cambrian time. The west side is horizontally displaced 5 km to the north and there has been rotation about a horizontal axis normal to the fault plane. The rotation produced relative vertical movement of the block such that near latitude 13° 03'S, longitude 130° 57'E, the throw is about 1500 m southeast block down, and just east of Manton Dam the throw is 620 m southeast block up.

At Mount Fitch there is evidence of minor faulting; however, there is little evidence that the Mount Fitch Fault Zone extends over the length indicated on the older geological maps (e.g. the Rum Jungle district 1:63 360 map).

2.7 Metamorphism

The effects of low-grade regional metamorphism are recognised in both the Lower Proterozoic sediments and the basement complexes. Higher metamorphic grade in dolomitic shales is locally associated with the Giants Reef Fault. All the Lower Proterozoic sediments are silicified and the quartz has been recrystallised.

Johnson (1974) believes that the boron and chlorine metasomatism seen in and around both complexes is evidence for renewed igneous activity in the basement complexes.

2.8 Mineralisation

All the economic uranium and base-metal orebodies in the Rum Jungle area occur within the interbasement syncline between the two complexes, This syncline was displaced by the Giants Reef Fault to form the embayment which contains Browns prospect and the Intermediate, Whites, and Dysons mines. The mineral deposits all occur in the Golden Dyke Formation close to the boundary with the underlying Coomalie Dolomite.

3. GEOPHYSICAL BACKGROUND

3.1 Gravity

Previous gravity investigations in the Rum Jungle area indicate a significant density contrast between the basement complexes and the surrounding metasediments. Similarly density measurements on core samples from the embayment area indicated a density contrast between the Coomalie Dolomite and the Golden Dyke Formation (Williams, 1970).

Previous gravity surveys: Previous gravity surveys conducted by BMR are summarised in Table 2. The surveys of Stott & Langron (1959) and Whitworth (1970) covered a large area and provide a regional gravity framework. Stott & Langron (1959) showed that gravity lows were produced by granites

in the Darwin-Katherine region. They observed negative anomalies of 12, 18, and 15 milligals over the Rum Jungle, Prices Springs, and Cullen Granites respectively, and suggested that the root of the Cullen Granite extends to 15 km. Other surveys were designed to look for orebodies or regional structure but showed that the Bouguer anomaly decreased from the sediments to the Waterhouse and Rum Jungle Complexes.

Detailed gravity surveys across the embayment and east of the Rum Jungle Complex provide important detail which was not obtained in the semi-regional coverage of the 1974 survey. Rock density measurements from the earlier surveys influenced the choice of densities used in interpreting the results of the 1974 survey.

3.2 Magnetics

Various ground and airborne magnetic surveys have been made in the Rum Jungle area. Early aeromagnetic work (Daly, 1957) showed large magnetic anomalies associated with the sediments in some areas. Small anomalies over the Rum Jungle and Waterhouse Complexes suggested that the Complexes may be composed of diverse and in some cases magnetic rocks.

In 1967 an area approximating the Hundred of Goyder was flown on east-west lines 160 m apart (Brown-Cooper & Gerdes, 1970). The area flown was from latitude 12^{o} 55'S to 13^{o} 7'S and from longitude 130^{o} 55'E to 131^{o} 09'E. This area covered the southern two-thirds of the Rum Jungle Complex and the northern third of the Waterhouse Complex. The results were contoured at an interval of 20 nT and show a variety of small magnetic features. A magnetic boundary which was initially described as a fault could possibly reflect the boundary between the Golden Dyke Formation and the Burrell Creek Formation.

Magnetic features in the complexes: Over the Rum Jungle Complex, only minor correlation is evident between the aeromagnetic results and Rhodes's (1965) rock subdivisions. Several small isolated anomalies in the Complex and on its eastern margin have been attributed to banded ironstone formations. Magnetic anomalies over the Waterhouse Complex suggest a variety of rock types in the complex with perhaps different densities for the different rocks.

Magnetic features in the sediments: Magnetic anomalies were observed in the sediments and appear to be due to amphibolite bodies containing pyrrhotite. Not all the amphibolite bodies are magnetic. The results of a ground magnetic survey (Daly, Horvath & Tate, 1962) showed that an amphibolite body near Brown's prospect had a variable magnetic susceptibility and an amphibolite investigated by Gardener (1971b) was non-magnetic. Williams (1970) explained a gravity high east of the Rum Jungle Complex as due to a non-magnetic amphibolite body.

3.3 Gamma spectrometry

An airborne gamma-spectrometer survey covering part of the Rum Jungle area is described by Beattie (1971). The response from the complexes was variable and might reflect the diverse rock types within the complex. However, widespread transported cover in this area precludes correlation of the results with buried rocks.

4. SURVEY DETAILS

4.1 Equipment

A description of the gravity meters, level, and micro-barometers used during the survey is given in Appendix 2.

4.2 Semi-regional survey

The Rum Jungle and Waterhouse Complexes and the surrounding metasediments were covered by 744 km of semi-regional traverses. The location of stations on the semi-regional traverses is shown in Plate 2. The traverse and station number code shown in Plate 2 is explained in Appendix 3.

Positioning of traverses: The traverses were positioned from airphotos at 1:25 000 scale and their positions were transferred to base maps, some at 1:25 000 scale and some at 1:50 000 scale. A north-south error in station location of ± 1 mm on the base maps would correspond to an error in latitude of 0.027' on the 1:50 000 maps and 0.013' on the 1:25 000 scale maps. These latitude errors produce errors in the Bouguer anomalies of 0.018 and 0.009 milligal respectively. In some areas positions could be located to better than this accuracy,,but in more featureless areas the errors in positions could have been as great as 2 mm.

Station spacing: Stations along the regional traverses were nominally 500 m apart. This distance was measured using odometers in the vehicles. In some places more detail was sought and the station spacing was reduced to 200 m or 250 m, and for these stations distances were chained.

Levelling of traverses: Surveyors from the Department of Services and Property pegged and levelled to third-order accuracy 471 km of regional traverses. The remaining 273 km of regional traverses were pegged and barometrically levelled by BMR personnel. The method of levelling the various traverses is indicated in Appendix 3. Station elevations are given in metres above Australian height datum (AHD) in Plate 2.

Levelling errors in the computed Bouguer anomaly at the surveyed stations were neglible but the levelling errors at barometrically levelled stations were significant.

Accuracy of barometric levels: The difference in air pressure between two stations at different heights is given by a complicated formula (Clark, 1953). This formula takes into account the lapse rate of the air column, the water vapour pressure, and the variation of gravity with latitude and altitude. The formula used for field reductions is given in Appendix 4 and was adapted from Clark's formula. The extra labour in applying the complicated formula is not justified because the mean of the temperatures measured at the two stations may be significantly different from the mean temperature of the air column whose weight the barometers measure. During the 1974 work the temperature was read only at the base station.

Appendix 4 demonstrates the dependence of errors in height on errors in temperature and errors in pressure. At a temperature of 300° K and for an elevation difference of 50 m between the base and station, the error in height due to an error in temperature is about 17 cm per degree Celcius. With a density of 2.67 g/m^3 for the Bouguer plate correction this corresponds to a Bouguer anomaly error of 0.033 milligal per degree Celsius. The microbarometers can be read to no more accuracy than ± 0.01 millibar, the hundredths being estimated. This pressure difference corresponds to a height change of ± 9 cm and an error in the Bouguer anomaly of ± 0.018 milligal.

In practice the errors in barometric levelling were greater than this. Before barometrically levelling any of the regional gravity stations a trial levelling survey was made at the spirit levelled stations along the Batchelor road. Figure 3 gives the results of these tests. Some of the barometric levels were out by two metres and the RMS error for all the observations was one metre; this corresponds to an RMS error of 0.2 milligal in the computed Bouguer anomalies. This error is acceptable if the results are contoured at one milligal intervals and the anomalies are large.

Gravity control network: Station 7408.0100 at the junction of the Stuart Highway and the Batchelor road was selected as the main base for the survey (see Appendix 3 for details of station locations). Fifty-five sub-bases were established during the survey by tying each new sub-base either to the main base or to an existing sub-base. If B1 represents a reading at an existing sub-base, and B2 represents a reading at the new sub-base whose observed gravity value is being sought, then the reading sequence was B1, B2, B1, B2, B1. This gave two values of B2 which had to agree to ± 0.03 milligal for an acceptable tie. Early in the survey these ties were all made with two gravity meters and generally the values obtained with both meters agreed to ± 0.02 milligal. Later, ties were made with only one meter.

Once the network of sub-bases was established, readings at the intermediate stations were made between hourly occupations of different sub-bases of reoccupations of the same sub-base. In this way station readings could be corrected for drift. Few of these intermediate stations were reoccupied. However, assuming the accuracy of ties between the sub-bases is representative of the reading accuracy for the other stations, the

observed values at these stations are probably within ± 0.05 milligal of their correct values. This error is small compared with the error introduced into the Bouguer anomaly values by barometric levelling.

4.3 Detailed traverses

In addition to the semi-regional traverses, 17 detailed traverses totalling 26 km were made over the Coomalie Dolomite/Golden Dyke Formation boundary to investigate the use of gravity to map the boundary. These traverses were positioned on airphotos and pegged by the Department of Services and Property surveyors. Gravity readings were made at 40 m station intervals and stations were levelled by BMR personnel using a Topcon automatic level. Misclosure of the levelled traverses was small (2 to 6 cm in 3 km) so errors due to levelling were probably negligible. The location of the detailed traverses is shown in Plate 1.

4.4 Density determinations

The density of core obtained during the 1974 drilling program was measured in the field using the displacement method. Further determinations using the same method were made in the laboratory on core from the 1973 and 1974 drilling program. Both the dry and saturated densities were measured. Mostly there was no significant difference between the two values because the core samples selected were fresh and had little porosity. The results of the dry determinations are given in Appendix 1 which also lists the results of susceptibility measurements of the core samples.

5. PRESENTATION OF RESULTS

The semi-regional gravity survey over the Rum Jungle and Waterhouse Complexes and surrounding sediments is presented as Bouguer anomaly contours in Plate 2 and as residual Bouguer anomaly contours in Plate 3. The detailed gravity traverses across the Coomalie Dolomite/Golden Dyke Formation boundary are presented as profiles in Figure 6 and 7.

5.1 Reduction of data

Instrument drift: All results were corrected for instrument drift. As shown in Section 4.2 drift corrections account for Bouguer anomaly errors of only ± 0.05 milligal.

Latitude corrections: All results were corrected for latitude using the station locations determined from airphotos. As shown in section 4.2 the latitude corrections introduce errors of less than 0.04 milligal in the Bouguer anomaly calculations.

Elevation corrections: Bouguer plate and free-air corrections were made at all stations.

The density used for the Bouguer plate correction was 2.67 g/cm^3, the average density for crustal material, and the density now adopted by BMR for regional reductions.

Williams (1970) used Nettleton's method over a hill of Acacia Gap Tongue and obtained a density of 2.6 g/cm^3 for use in calculating the Bouguer anomaly. Unfortunately this hill, like many others in the area, owes its existence to an outcrop of unusual lithology so this density value may not be representative of other formations.

In the Rum Jungle area the relative errors in the Bouguer anomaly map due to a wrong choice of density would be negligible because the height variations are small. Even the steepest slopes are associated with height changes of only 100 m. With this extreme change, an error of 0.1 g/cm^3 would produce an error of only 0.4 milligal.

As shown in Section 4.2 the elevation corrections are subject to errors of ± 0.2 milligal due to barometric levelling errors.

5.2 Tying of survey to Isogal network

At the end of the survey the gravity reading at Station 7408.0100 was tied to bench-mark SH55 about 1 km south of the junction of the Stuart Highway and the Batchelor road. This bench-mark has BMR gravity station number 6007.5055 and the observed gravity value is 978 322.04 milligals. This station, in turn, had been tied to the Isogal network. The observed value obtained for station 7408.0100 using this tie was 978 318.95 milligals (Station 7408.0100 has the field identifier AA0.0 and is at the junction of the Batchelor road and the Stuart Highway).

5.3 Removal of regional gradient

Whitworth (1970) has described the regional gravity features in the Northern Territory and shows that the survey area lies near the boundary between the Tipperary Regional Gravity Low and the Marrakai Gravity Plateau. The gravity low is due to the lighter Palaeozoic sediments of the Daly River Basin, and the gravity plateau is due to the heavier Lower Proterozoic sediments of the Pine Creek Geosyncline. The regional gradient observed in the survey area is due to the increase in gravity from the gravity low to the gravity plateau. This gradient has been largely removed in Plate 3 by scaling a regional gradient from the 1:250 000 preliminary Bouguer anomaly mapeproduced from the reconnaissance helicopter gravity data. This regional gradient was approximated as a plane surface rising from the southwest to the northeast corners of the anomaly map. This plane had a west to east gradient of $\pm$ 0.46 milligal per minute of longitude and a south to north gradient of $\pm$ 0.57 milligal per minute of latitude. The linear gradients were removed from the Bouguer anomaly map (Plate 2) to give the map of Plate 3. Comparison of the maps shows that most of the regional gradient has been removed by this method.

6. DENSITY MEASUREMENTS

The densities of rocks in the Rum Jungle area were determined from the results of previous gravity surveys and measurements on 67 samples of drill core from the 1973 and 1974 BMR drilling programs in the area. The results of density determinations on the 1973 and 1974 core samples are presented as histograms in Figure 4. Three broad groups of rock densities are recognised. The first group of low-density rocks comprise the low-

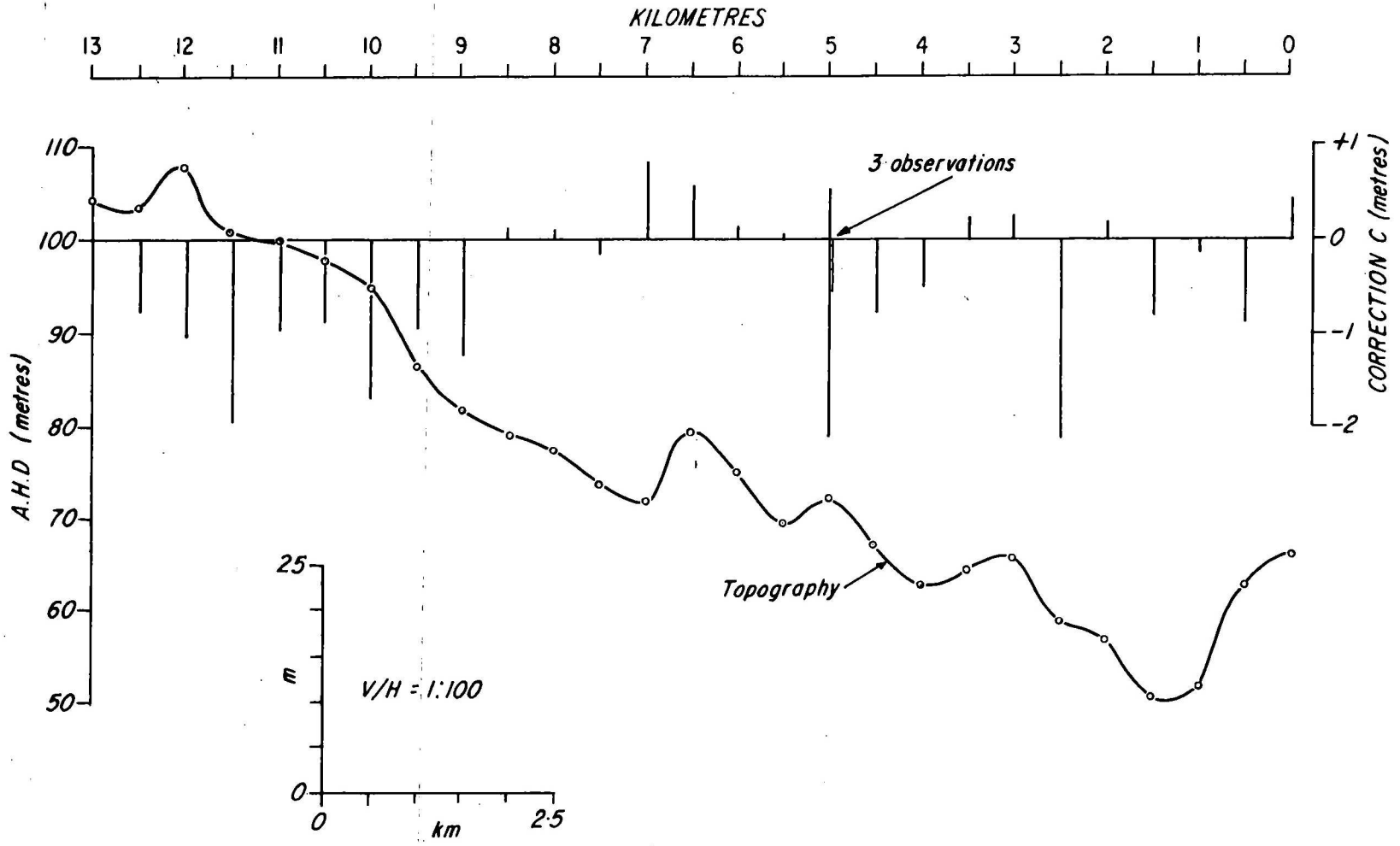

Correction C = Spirit levelled height – barometrically levelled height

R.M.S. correction = 1 metre

RESULTS OF BAROMETRIC LEVELLING TEST TRAVERSE AB (BATCHEOR ROAD)

Fig. 3

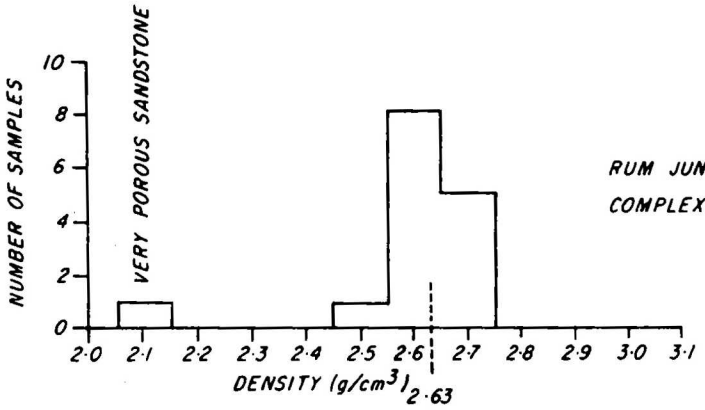

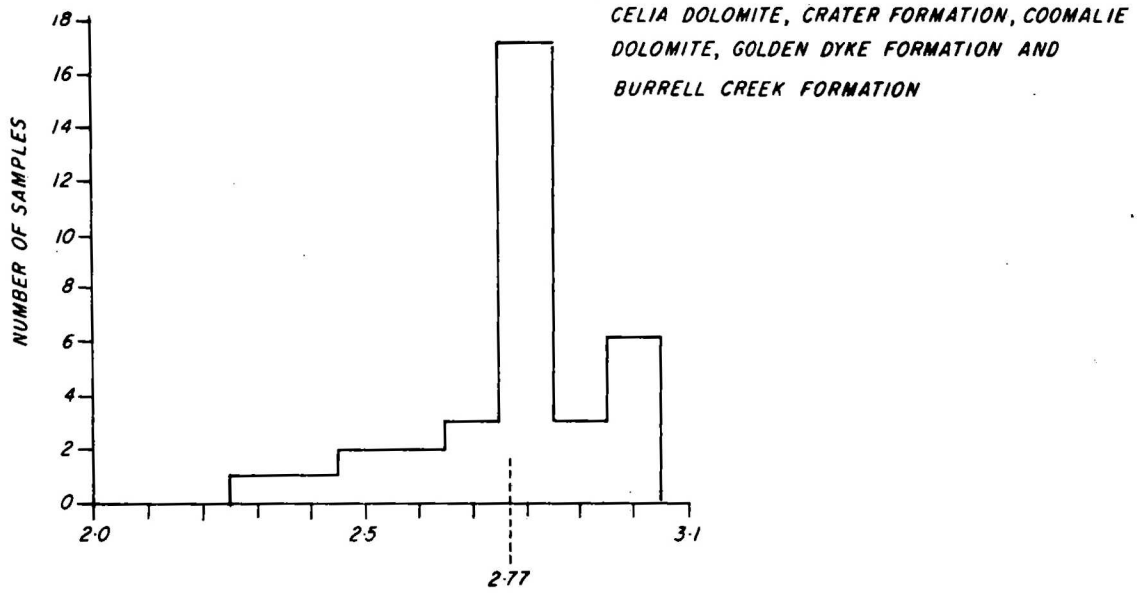

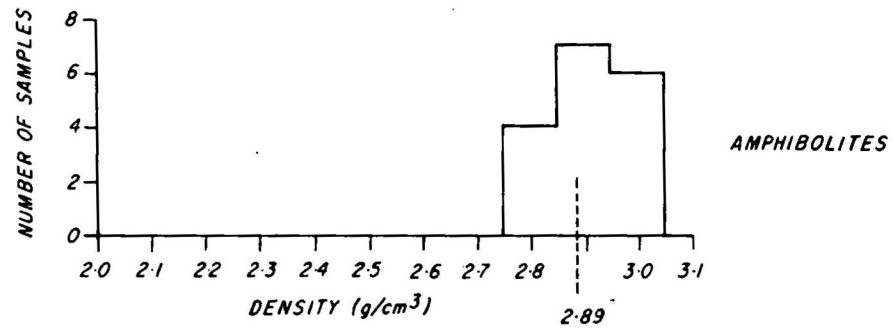

HISTOGRAMS OF ROCK DENSITY

density parts of the basement complexes and the Beestons Formation which directly overlies the complexes. The low-density group is thought to represent the gross distribution of low-density material in the area. Note that not all rocks in the complexes are of low density. Celia Dolomite, Crater Formation, Coomalie Dolomite, Golden Dyke Formation, and Burrell Creek Formation form a second group of rocks with intermediate densities. This second group is thought to represent the average density of sediments in the area. The amphibolite bodies were included as a third group of high-density material. Amphibolite occurs in the Golden Dyke Formation, Coomalie Dolomite, and Celia Dolomite. Its density is high, so that if sufficient amphibolite is present it will produce recognisable gravity highs.

The results of density measurements made on the 1973 and 1974 core samples plus the densities determined by Langron (1956), Daly, Horvath & Tate (1962), and Williams (1970) are compared in Figure 5. This figure also shows the density values which were adopted for modelling and interpretation of the gravity survey results.

7. MAPPING THE COOMALIE DOLOMITE-GOLDEN DYKE FORMATION BOUNDARY

Seventeen detailed gravity traverses were made to determine if gravity could be used to map the economically significant boundary between Coomalie Dolomite and Golden Dyke Formation. The location of the traverses is shown in Plate 1. Figures 6 and 7 show the results of the detailed traverses as Bouguer anomaly profiles and the geological boundaries, determined by electrical geophysics (Ogilvy, in prep.), gravity, and geology.

On some traverses there is a discrepancy between the geological boundaries shown on the profiles and those in the solid geology map. The latter boundaries are approximate only. The geological legend for the symbols in Figures 6 and 7 is identical with the legend shown in Plate 1.

Record No. 1977/9

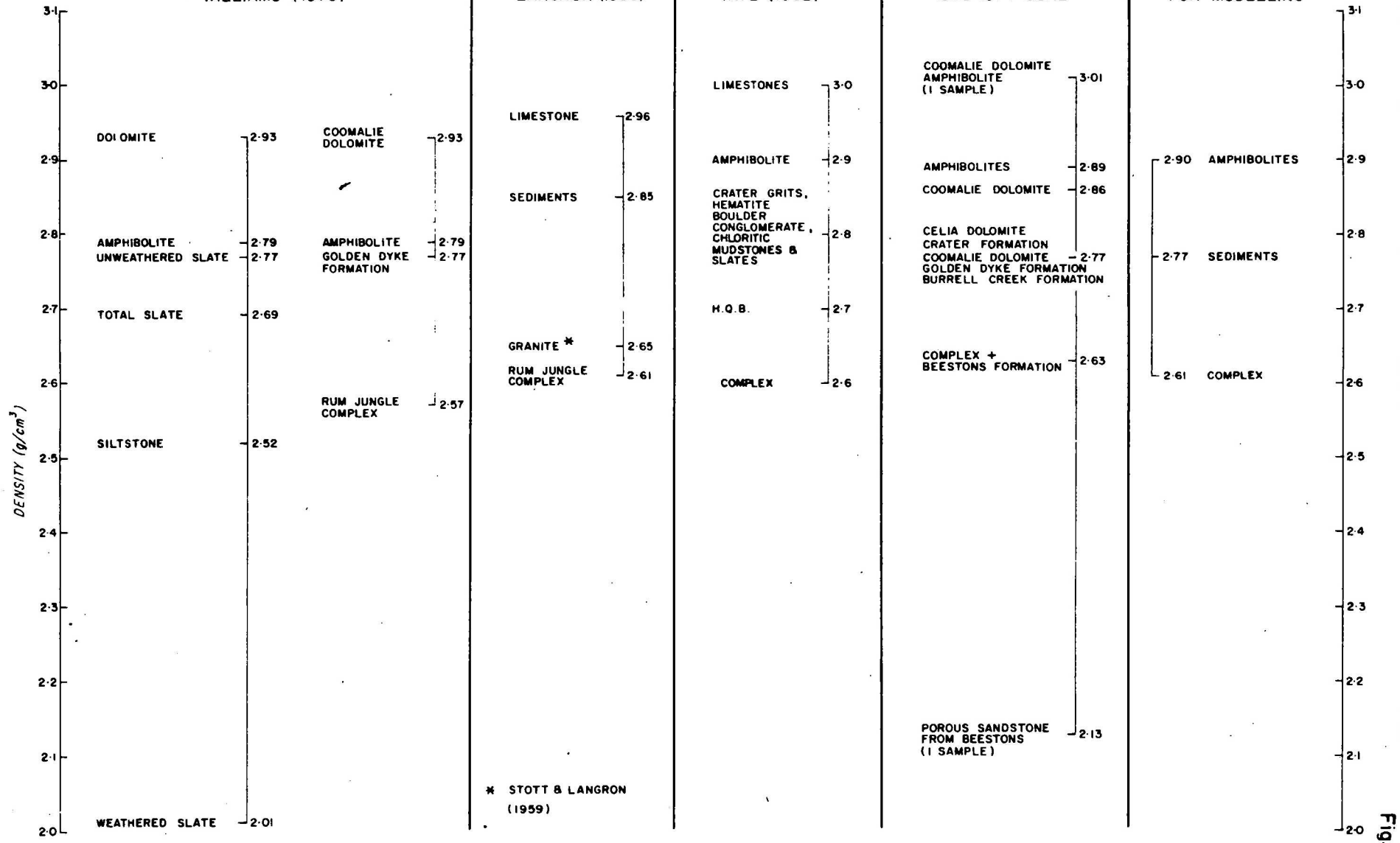

SUMMARY OF
DENSITY MEASUREMENTS

Fig. 5

D52/B7-672A

Fig. 6

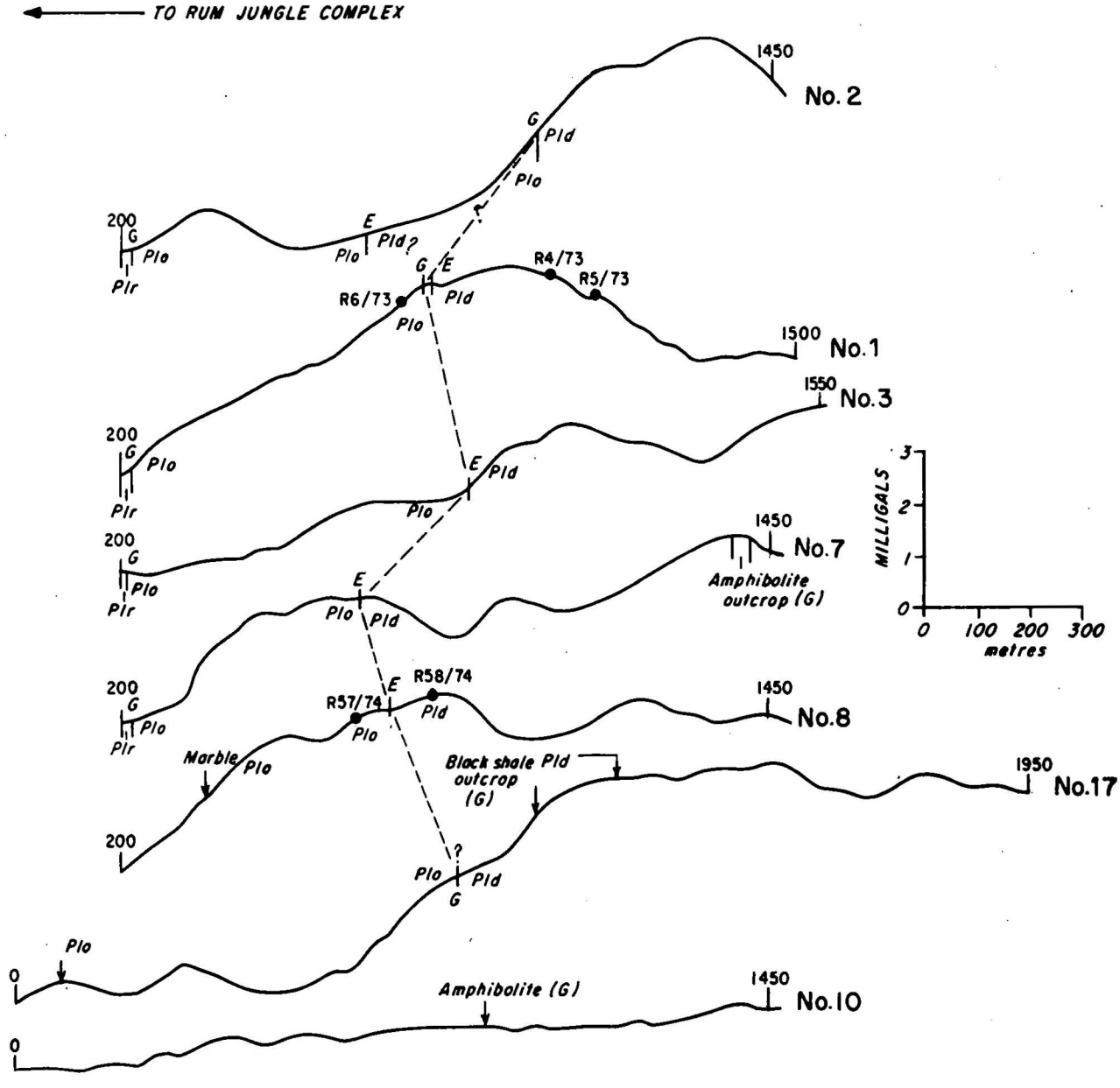

G From geological data

E From electrical geophysical data

? Boundary doubtful

• Drill hole

DETAILED GRAVITY PROFILES SOUTH OF RUM JUNGLE COMPLEX

Fig.7

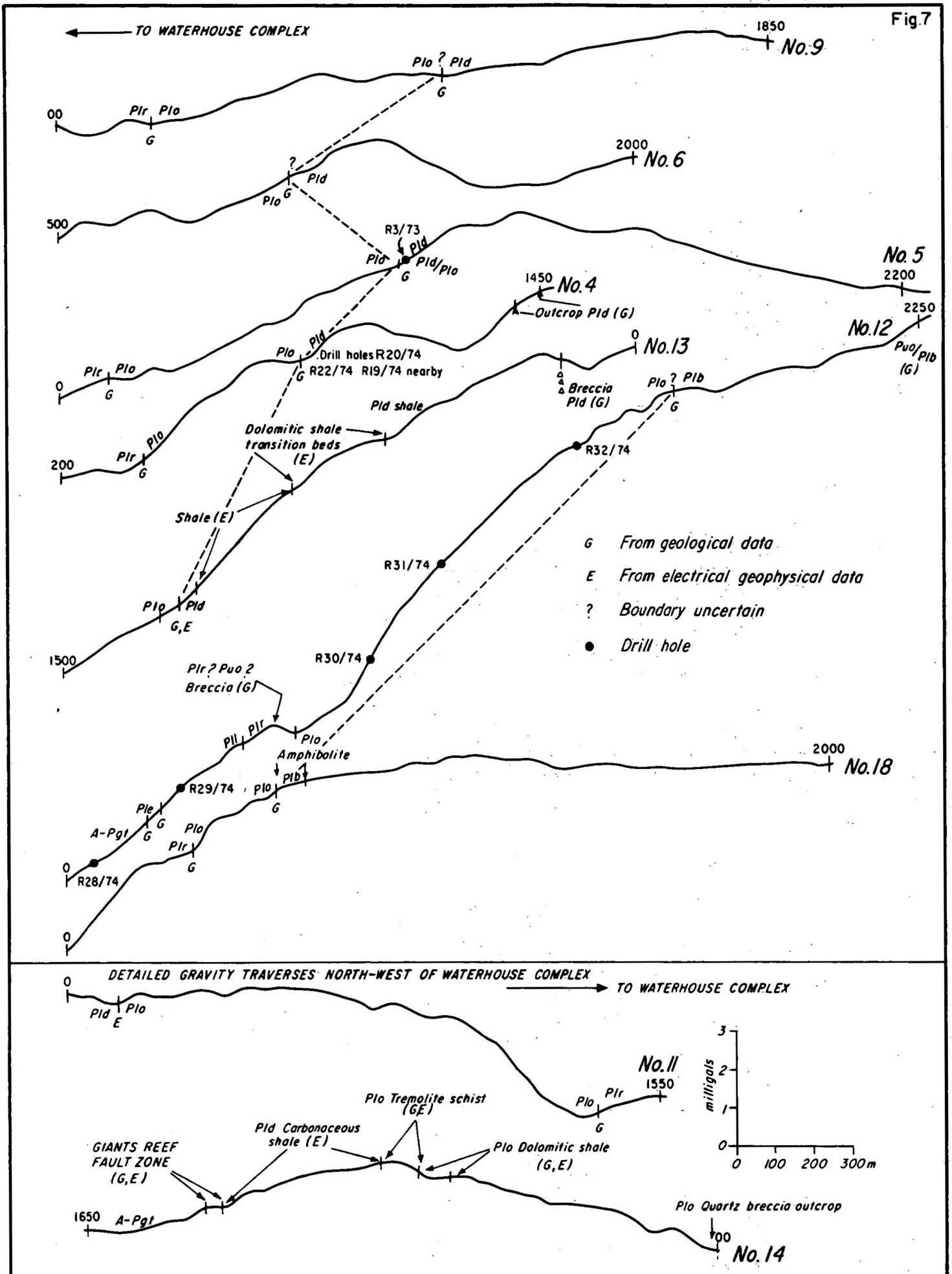

DETAILED GRAVITY PROFILES AROUND THE WATERHOUSE COMPLEX

Record No. 1977/9

D52/B7-656A

Examination of the profiles reveals that the gravity method cannot be used to map the Coomalie Dolomite/Golden Dyke Formation boundary. The boundary is in many places gradational and the transition zone, mapped as Golden Dyke Formation, contains amphibolite and carbonaceous calcareous shale which have similar densities to unweathered dolomite. Both formations contain amphibolite bodies so that dense amphibolite is not diagnostic of a particular formation. In short, there is no clear density contrast between these formations.

On traverses 2, 1, and 3, and to a lesser extent traverse 8, there is a gravity high over the Golden Dyke Formation adjacent to the boundary. On traverse 7 the gravity high is common to both formations. The cause of the high is unknown. Drill-holes R6/73 on traverse 1 and R57/74 on traverse 8 encountered dolomitic marble of density 2.98 and 2.95 g/cm^3 respectively. Holes R4/73 and R5/73 (traverse) encountered calcareous carbonaceous pyritic shale of density 2.80 g/cm^3 which is only 0.03 g/cm^3 higher than the average vlaue assumed for the sediments. None of these holes exceeded 55 m depth, and the source of this gravity high could lie below the depth of drilling.

William's (1970) work showed that gravity lows occur over the Celia and Coomalie Dolomites; this could be due to extensive silicification, weathering, or fissuring. These features would lower the density below that observed in the unweathered specimens of drill core. No consistent correlation of gravity lows with Coomalie Dolomite was observed in the 1974 results. Traverses 2 and 17 show the gravity decreasing onto the Coomalie Dolomite; however, this decrease is partly due to the less dense Rum Jungle Complex to the north. The gravity lows observed by Williams (1970) over the Celia Dolomite are sharp and can be separated from the broader low due to the Rum Jungle Complex. They can be explained by material of density contrast -0.2 g/cm^3 extending from the surface to 300 m deep.

Traverses 9, 6, 5, 4, and 13 (Fig. 7) show no gravity effect directly attributable to the Coomalie Dolomite/Golden Dyke Formation boundary. On traverses 4 and 5 a gravity high occurs in the Golden Dyke Formation adjacent to the boundary. The boundary on traverse 6 was inferred from gravity data alone and was simply marked on the western flank of the gravity high.

On traverses 12 and 18 there was no gravity feature associated with the boundary between the Coomalie Dolomite and Burrell Creek Formation.

Traverses 11 and 14 both show the gravity decreasing towards the Waterhouse Complex but there is no feature associated with the Coomalie Dolomite/Golden Dyke Formation boundary. The gravity low on traverse 11 at about 1350 m may be due to weathering of the dolomite. A similar low, also adjacent to the Crater Formation/Coomalie Dolomite boundary, occurs on traverse 12. On traverse 14 the gravity low extending from the Giants Reef Fault zone to 1670 m is caused by an inlier of Waterhouse Complex. This low is evident on the semi-regional contour maps (Plates 2 and 3).

8. RESULTS OF SEMI-REGIONAL SURVEY

The residual Bouguer anomaly contour map (Plate 3) shows a flat and smooth gravity profile over the metasediments and gravity lows associated with the basement complexes. The gravity results over the metasediments suggest that the metasediments are thick and have a generally uniform density. The gravity lows over the complexes suggest that the complexes contain a considerable volume of low-density material. However, two gravity lows are observed over the Rum Jungle Complex and indicate that the complex is composed of at least two different rock types with different densities.

8.1 Correlation of gravity and geology in the Rum Jungle Complex

The gravity results over the Rum Jungle Complex have only rough correlations with Rhodes's subdivisions (Fig. 2). The local high at 12°58'S, 131°04'E coincides roughly with the schists and gneisses, whereas the local low at 12°59'S, 131°04'E surrounds a small outcrop of leucocratic granite but is much more extensive than the mapped outcrop. Because the leucocratic granite is the youngest member of the complex one is tempted to identify it with the low-density diapiric intrusive granite postulated by Stephansson & Johnson (1975). However known outcrops of leucocratic granite are not always associated with gravity lows, and vice versa. (For example at 12°58'S, 130°58'E and 12°55½'S 131°05'E).

The southern gravity low at $13^{o}01'S$, $131^{o}01'E$ lies mainly in the area mapped as coarse granite and large feldspar granite. Within this low there is a small outcrop of leucocratic granite which possibly represents the top of a low-density dome which produces the gravity low.

The northern low centred at $12^{o}52'S$, $131^{o}04'E$ lies almost on the complex/sediment boundary and suggests that low-density material extends beneath the sediments. Rhodes shows metasediments at the centre of the low, and leucocratic granite extending to the east and southeast. The leucocratic granite outcrop corresponds to the trend of the gravity trough, and suggests that the leucocratic granite has a low density.

8.2 Correlation of gravity and geology in the Waterhouse Complex

No geological subdivisions are available for the Waterhouse Complex, but the gravity picture is simpler and indicates that there is probably only one centre of low-density material.

The gravity low at $13^{o}02'S$, $130^{o}57'E$ is due to a part of the Waterhouse Complex apparently displaced by the Giants Reef Fault. The deficient mass of material producing this low is 3.5×10^{14}g and, assuming a density contrast of 0.16 g/cm^3, the body has a volume of 2.2 km^3. The surface area of the body is 1.7 km^2 and with a mass distribution in the form of a vertical cylinder, the depth extent is 1.3 km. The surface geological dips of the Crater Formation indicate that the body broadens with depth, so the base is probably less than 1.3 km below the surface.

8.3 Correlation of gravity and geology in the metasediments

The gravity low extending east of the Waterhouse Complex at $13^{o}05'S$ is probably due to a shelf of low-density material dipping gently east from the complex.

The cause of the gravity ridge around the southeastern side of the Waterhouse Complex is not known. This ridge continues north-northeast from Burrell Creek Formation at $13^{o}12'S$ to Golden Dyke Formation at $13^{o}7'S$.

8.4 Other correlation of gravity and geology

The Giants Reef Fault is apparent from the gravity contours where it has faulted the Rum Jungle Complex to form the embayment and where it has sheared material from the Waterhouse Complex to produce the gravity low at 13°02'S, 130°57'E. Elsewhere there is no expression of the fault. This is not surprising where sediment has been faulted against sediment or complex against complex; but it is surprising to see no strong gravity gradient associated with the fault on the eastern margin of the Rum Jungle Complex where the fault separates the complex and sediments. The absence of a gravity gradient across the fault in this area suggests that parts of the complex and sediments have the same density. Another interesting feature of this eastern margin of the Rum Jungle Complex is that the steepest gradients do not coincide with the fault and suggest that low-density material continues at depth to the southeast of the fault.

The source of the small gravity high at 13°00'S, 130°58'E is not known. It occurs over Coomalie Dolomite opposite the embayment and could be caused by amphibolite within the dolomite.

Another small high of unknown origin is at 12°57'S, 131°07'E over the Golden Dyke Formation and is probably due to amphibolite. This high shows up in Williams's (1970) work. Williams also found a more intense high about 4 km further west over an amphibolite body, but no readings were made in this location during the current survey.

There is a small high at 13°02'S, 131°05'E over Celia Dolomite and a small low at 13°09'S, 131°01'E close to the Coomalie Dolomite/Golden Dyke Formation boundary. The source of both these features is not known.

9. INTERPRETATION OF SEMI-REGIONAL SURVEY

To better understand the relations between the gravity results and the geology of the Rum Jungle area, the geometry and density of the rocks giving rise to the gravity features were investigated by gravity modelling and determinations of excess mass.

9.1 Problems in gravity modelling

In gravity modelling the response of theoretical models is calculated and compared with the gravity results obtained by field work. However, as there is an inherent ambiguity in the solution to the mass distribution producing a known gravitational field, a match between theoretical and field results is not a sufficient test of the validity of a model.

The ambiguity of interpretations based on gravity modelling is illustrated in Figure 8 which shows some of the models that might be used to generate the gravity lows observed over the basement complexes at Rum Jungle.

The models show that quite different bodies of low-density material embedded in rocks of a higher density can be made to fit the same observed gravity profiles. The first model shows the low-density material being undercut and forming a thin layer near the surface in the areas of the Complex not having a marked gravity low. The second model shows the low-density material in the form of a wedge, so that in areas of the Complex without marked gravity lows the material is thin and at depth. A third model, intermediate between the other two, shows the low-density material lensing out from above and below.

As a check on the validity of a model which matches field results it is possible to use unambiguous depth estimates and tests of geological feasibility. Depth estimate controls are provided by the fact that it is possible to estimate a maximum depth to a source: sharp features in a gravity profile indicate near-surface sources. A test of geological feasibility is provided by the fact that most granites are in the form of batholiths whose sides dip outwards at steep angles. This condition favours the second model shown in Figure 8. Stephansson & Johnson (1975) suggest that both the Rum Jungle and the Waterhouse Complexes have been intruded by low-density granitic material in the form of domes, and this also favours the second distribution.

9.2 Densities used for modelling

Measurements on drill core (Fig. 4) indicate that a density of 2.61 g/cm^3 can be assigned to the low-density material in the basement complexes. This figure may even be too low for granites, which have a mean density of 2.67 g/cm^3.

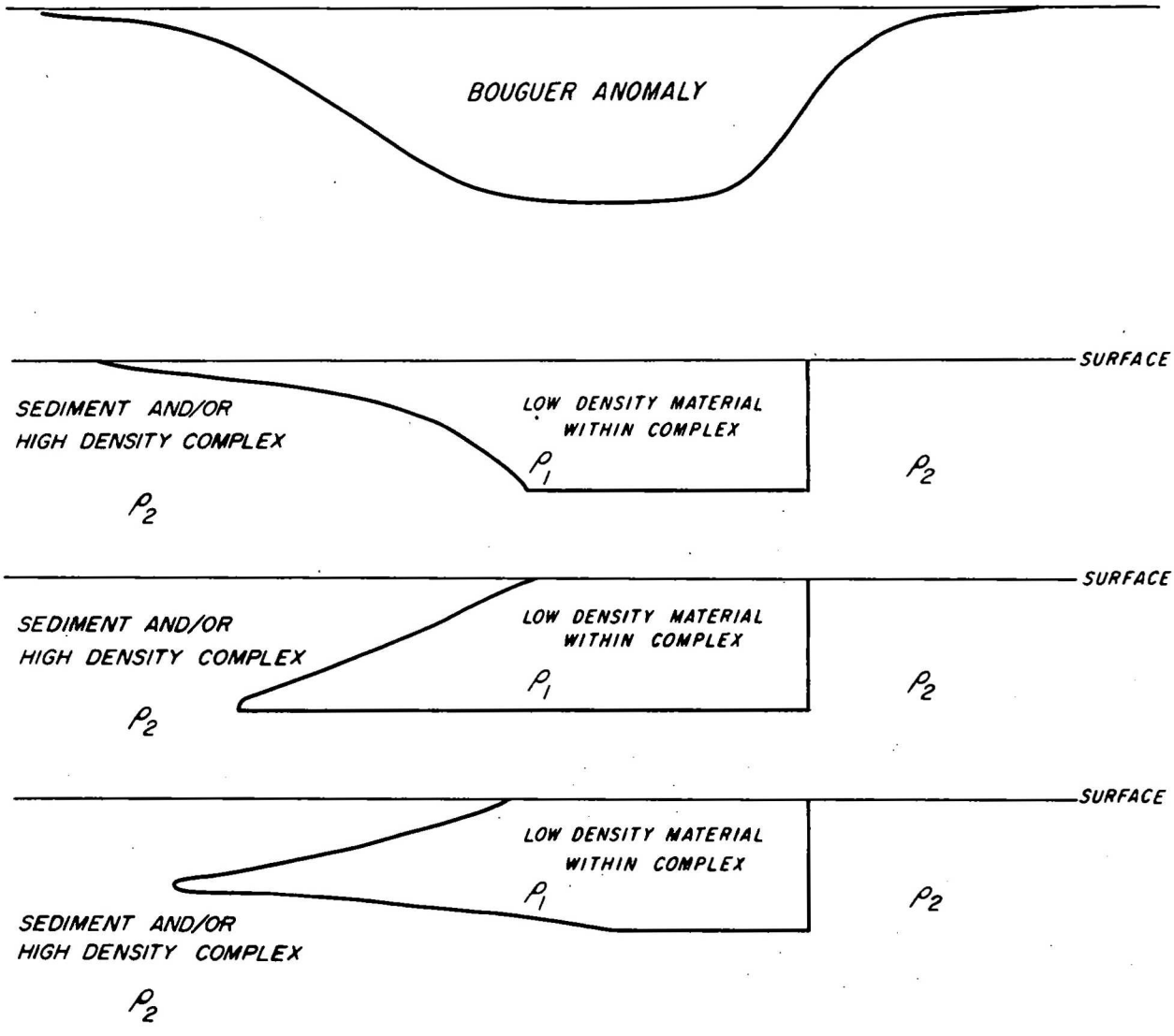

POSSIBLE DENSITY DISTRIBUTIONS TO PRODUCE GRAVITY LOWS

(not to scale)

No density measurements on drill core were available for the higher-density component of the complexes, but this was given a density equal to that of the metasediments. The main reason for this choice comes from a gravity traverse which crosses the Giants Reef Fault and indicates that there is little density contrast between this part of the complex and the metasediments. Geological evidence indicates there are at least 400 m of sediments east of the fault, and if a density contrast of 0.16 g/cm^3 existed between the Complex and the sediments this would produce a change of 2 milligals per km within 0.5 km either side of the fault. No such change was observed; there are only small fluctuations of 0.3 milligal across the fault and these are probably superficial in origin. There are also other places where there is little change across the boundary between the Rum Jungle Complex and metasediments, for example along 12^{o}55'S across the western boundary of the complex, where the geological dips are 60^o.

Hence on the basis of density measurements and field observations it seems necessary to consider only three rock densities in the survey area. These densities and the rocks with which they are associated are:

2.61 g/cm^3 for the low-density material of the complexes and the Beestons Formation;

2.77 g/cm^3 for the remainder of the complexes and the metasediments;

2.90 g/cm^3 for the amphibolite bodies.

9.3 Modelling of complexes

Two-dimensional models were used to investigate the geometry and density of the basement complexes. Models were generated to match residual Bouguer anomaly profiles obtained over the basement complexes. The Bouguer anomaly profiles were obtained from the contour map of Plate 3. The locations of the profiles are shown in Plates 1 and 3.

The modelling is based on the following assumptions:

(a) the metasediments and high-density rocks of the complexes have a uniform density of 2.77 g/cm^3;

(b) gravity lows are caused by homogeneous material with a density of 2.61 g/cm^3 in the basement complexes;

(c) small gravity highs are caused by small bodies of amphibolite or dolomite;

(d) there are no lateral density contrasts in the rocks underlying theccomplexes and metasediments;

(e) the rocks underlying the complexes and metasediments probably comprise a sub-basement having a density of approximately 2.67 g/cm^3 (crustal average);

(f) the low-density rocks of the complex probably grade into the sub-basement at depth.

The assumption of a laterally uniform sub-basement means that we need only model the density contrast between the low-density rocks of the complex and the high-density metasediments and complex rocks. The modelling is carried out by embedding models of low-density material (the low-density rocks of the complex) in a homogeneous host of high density (the metasediments and high-density rocks of the complexes). The assumption that the low-density rocks of the complex grade into the uniform sub-basement implies that the depth extent of the low-density models is more representative of the thickness of the sediments than of the low-density parts of the complexes.

Owing to the large size of many of the sources modelled, two-dimensional modelling provides an adequate representation of most geological sources. However, when the dimensions of sources were short, three-dimensional modelling was used to check the validity of the two-dimensional models.

Profile C-C': Figure 9 shows the observed and calculated gravity profiles along C-C' through the Waterhouse Complex. The model represents a two-dimensional distribution of low-density material in the Waterhouse Complex. When the outcrop of the model is compared with the known geology along the profile one feature is evident: not all of the Waterhouse Complex comprises low-density material.

Record No. 1972/9

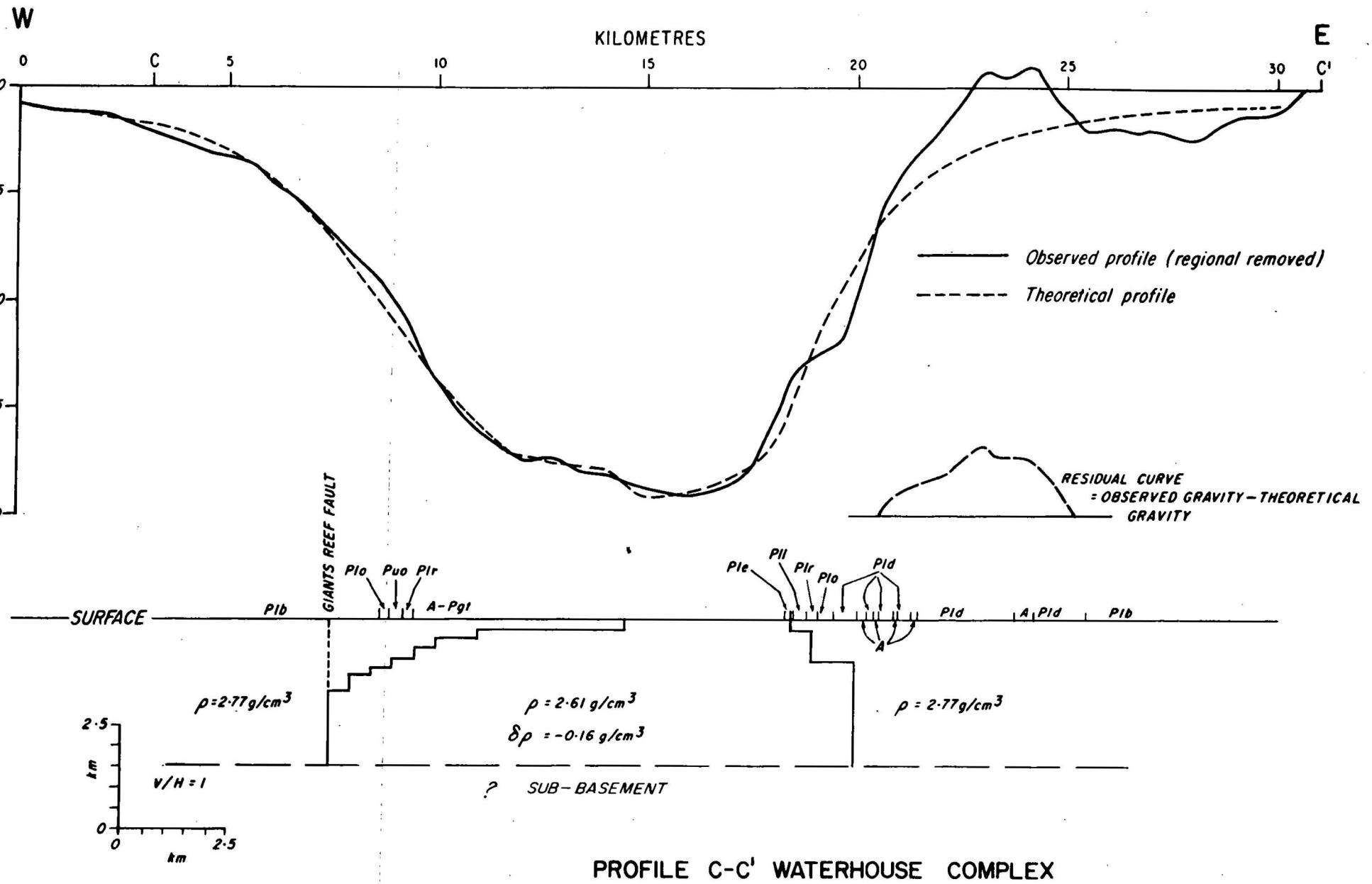

PROFILE C-C' WATERHOUSE COMPLEX

D52/B7-658A

Fig. 9

The validity of the cross-section used in the two-dimensional modelling of the Bouguer anomaly along traverse C-C' is illustrated in Figure 10. This plate shows the similarity of the gravity profiles calculated for three low-density bodies which have similar cross-sections to the two-dimensional model shown in Plate 8 but different strike lengths. The strike length of the finite bodies is 8 km north and south of traverse C-C' and was estimated from the geological boundaries shown in Plate 1. The lower curve corresponds to the anomaly produced by a rectangular two-dimensional body of depth extent 3.5 km. The upper curve is produced by a body of the same cross-section but which extends o only 8 km north and south of the traverse. The central curve shows the anomaly over a rectangular block of material extending 8 km north and south of the traverse and to a depth of 3.7 km.

The main feature of the two-dimensional model is that the depth extent of the low-density model (and hence the depth extent of the metasediments) is 3.5 km. Although this depth estimate is based on a two-dimensional model the exercise in three-dimensional modelling shown in Figure 10 indicates that the thickness of the metasediments is probably no greater than 4 km. The estimated maximum depth of 4 km assumed that the density contrast is no smaller than 0.16 g/cm^3. If the low-density rocks of the complex grade into higher-density rocks at depth as is proposed, then the estimate of the thickness of the sediments would be increased.

A residual high observed on the field profile at 23 km is not accounted for by the simple model used. This high of about 3 milligals is an extension of a ridge of high gravity skirting the southeast flank of the Waterhouse Complex. The cause of this high is not known. Amphibolite is mapped on the traverse; however, there is not sufficient shown to account for the residual gravity high. If we assume the residual high is due to a two-dimensional body of density contrast +0.13 g/cm^3 then the cross-sectional area of the body would have to be about 1.7 km^2. This is about the same size as the amphibolite body of 2.2 km^2 cross-sectional area postulated by Williams (1970) east of the Rum Jungle Complex.

Fig. 10

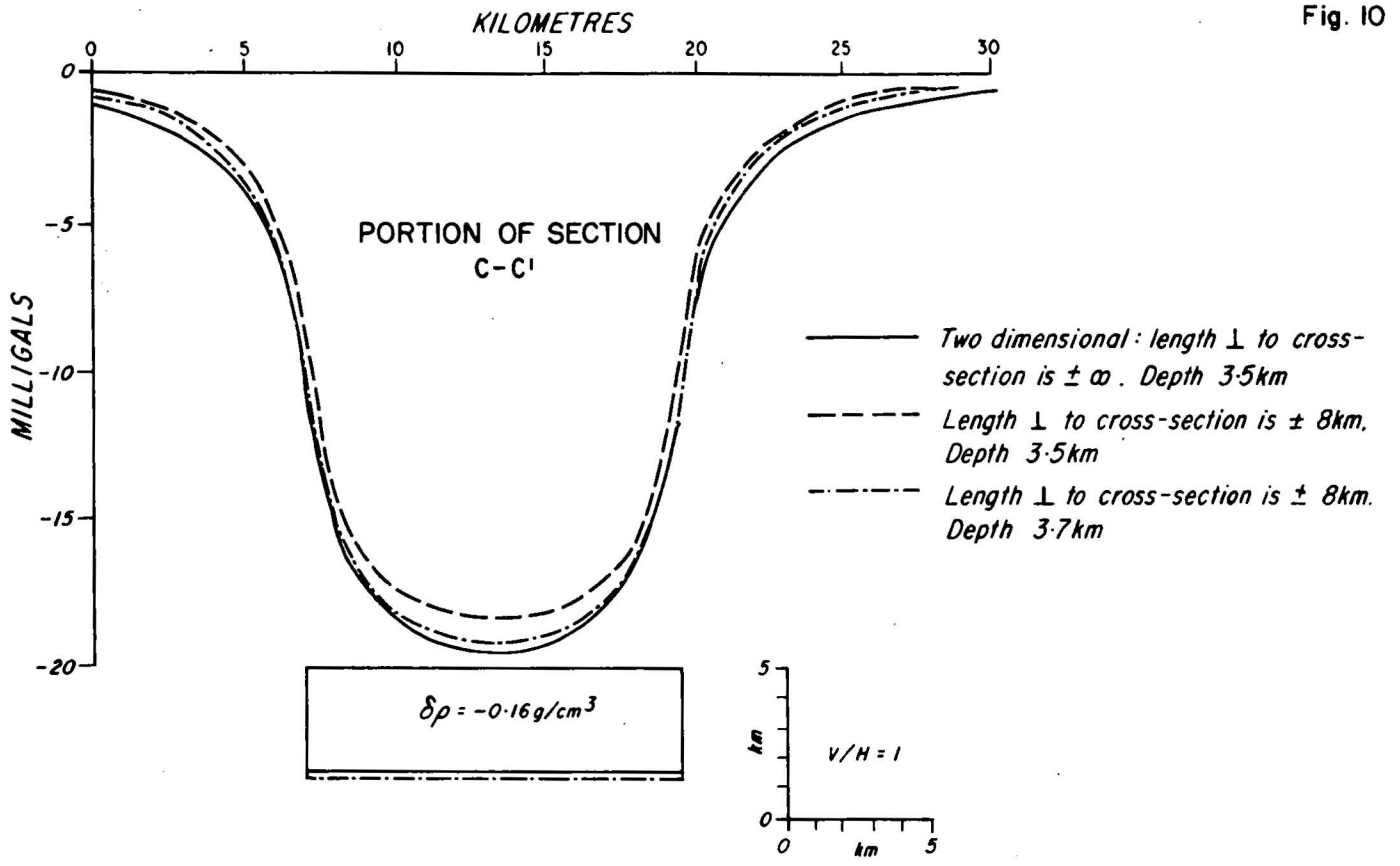

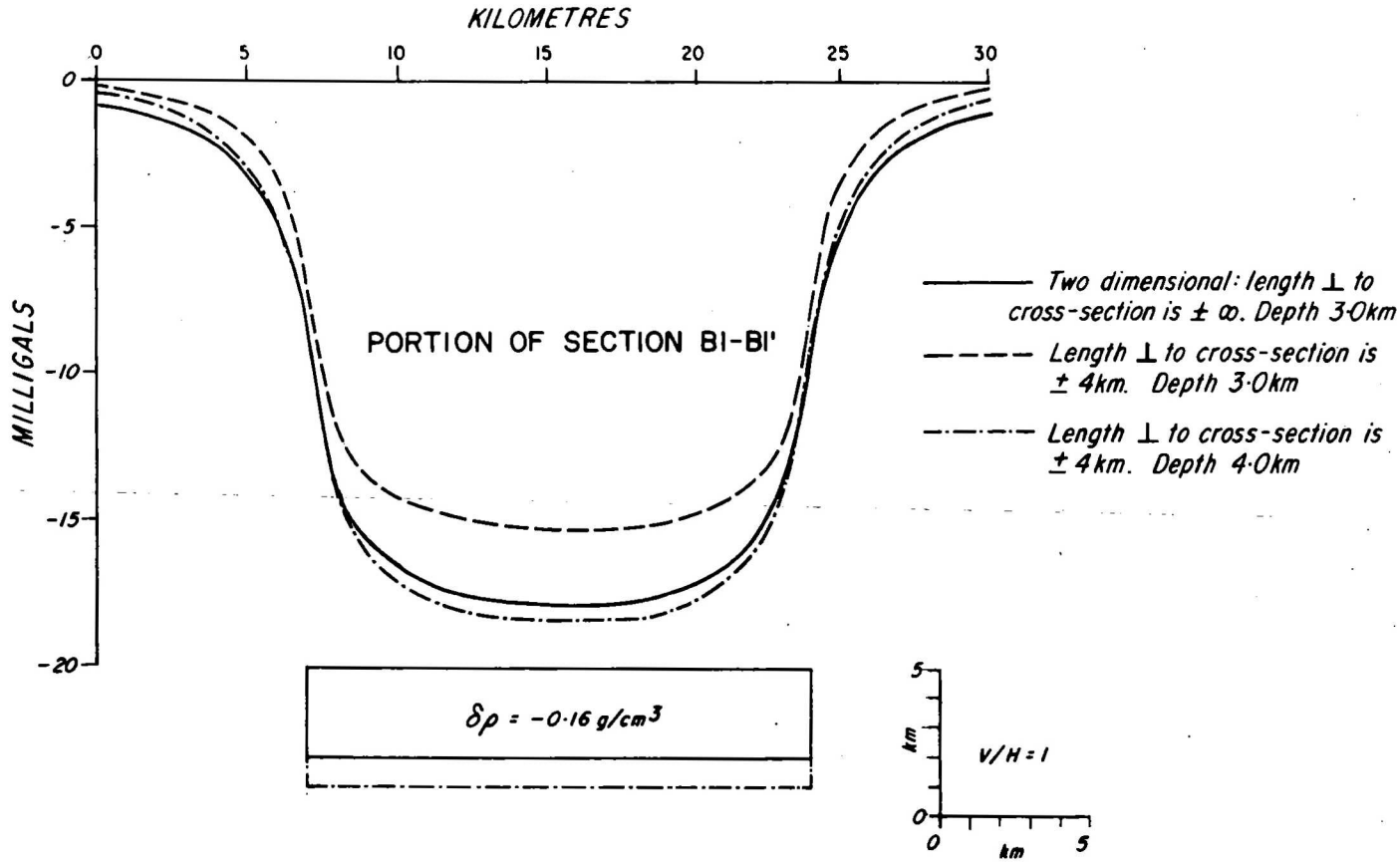

COMPARISON OF TWO AND THREE-DIMENSIONAL MODELS

Profile B1-B1''': Plate 4 shows the observed and calculated gravity profiles along the B1-B1'-B1''-B1''' from south of the Waterhouse Complex to north of the Rum Jungle Complex. Two possible models are given; the first shows a low-density model extending to 3 km depth with the depth to the top surface varying. The second model has both the top and the bottom at a variety of depths. The first model is consistent with Stephansson & Johnson's (1975) idea of dome-like intrusive structures. The second model, although giving a slightly better fit to the observed curve between 36 and 45 km, requires the body to decrease in width from above and below at 40 km. This distribution has no geological backing as it requires high-density material to underly the low-density rocks of the complex.

A peculiar feature of the observed profile is a sharp corner at 4 km. This can only be due to a near-surface feature. The profile shape suggests that the light material is in the form of a wedge as shown in Figure 11. This seems unlikely because the light material in this model is at the surface and extends 0.65 km beyond the complex/sediment boundary. This model is not geologically satisfactory and model No. 1 (Plate 4) may better represent the distribution of light material. The discrepancy between the observed and calculated profile at this southern end could be due to dense material (amphibolite?) in the sediment as was proposed for the anomaly on profile C-C'.

The trough of sediments between the complexes is shown extending to 3 km and 2.75 km respectively in models No. 1 and 2. Figure 12 is part of the profile A-A' which closely parallels B1'-B1'' over the sedimentary trough between the complexes. In this model the sediments are shown extending to 2.65 km. This assumes a two-dimensional cross-section and since the dense sediments appear to increase in cross-section on both sides of this profile, the model probably represents a maximum depth of sediments along profile A-A'.

The effect of assuming infinite strike length perpendicular to the profile introduces a greater error in depth on profile B1-B1' than on C-C'. This is because the width of the complexes along traverse B1-B1''' seldom exceeds four kilometres in both directions. Figure 10 shows the gravity profiles over several rectangular blocks which model the density contrast between the Waterhouse Complex and the metasediments along profile

Record No. 1977/9

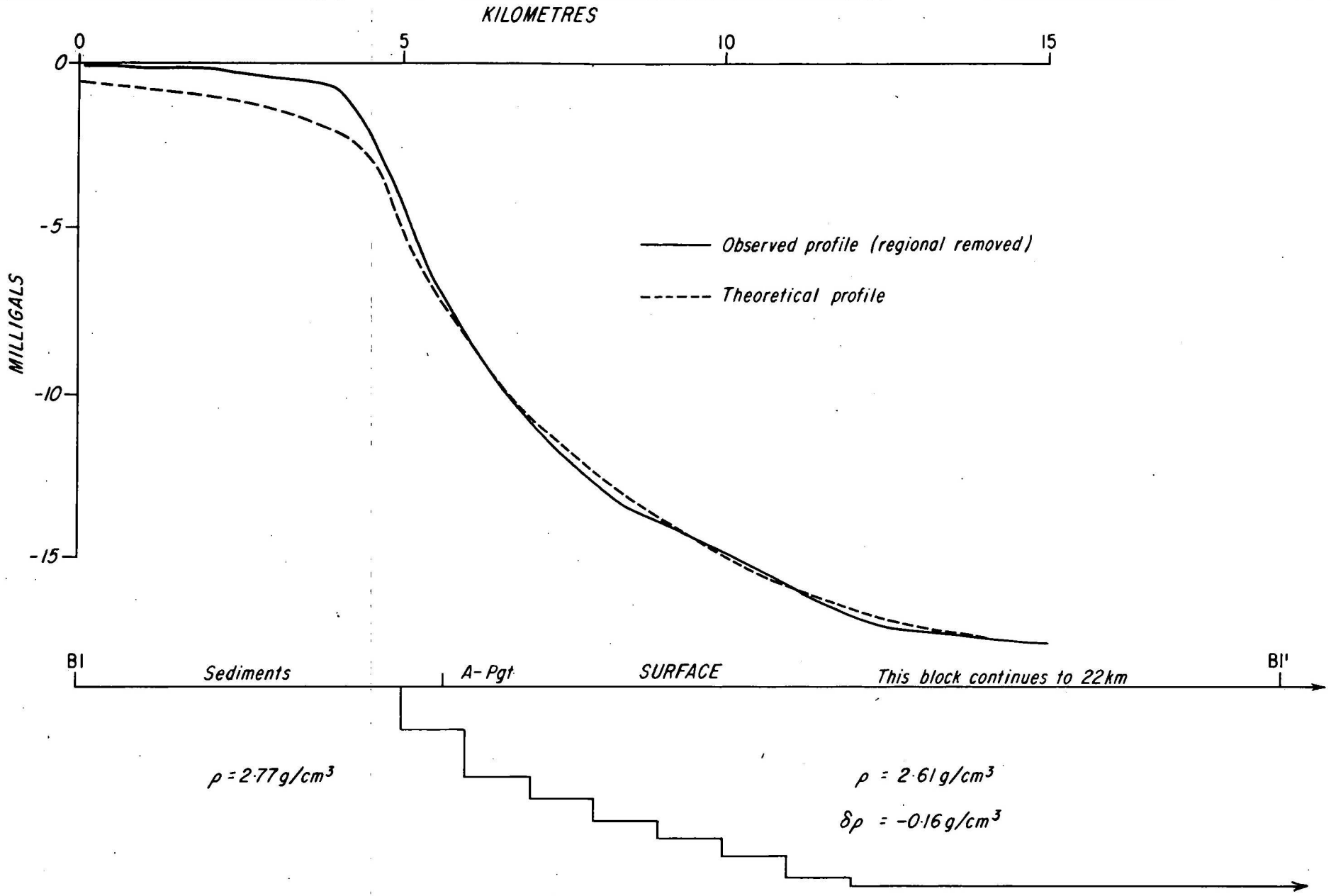

ALTERNATIVE MODEL ON B1–B1' WATERHOUSE COMPLEX

Fig 11

D52/B7-661A

block. The upper profile is drawn for the same cross-section but with the extent of the block reduced to four kilometres either side of the traverse. The anomaly has decreased by about 2.8 milligals. The lower profile is the anomaly over a block 17 km, by 4 km either side of the traverse, by 4 km deep. The additional one kilometre depth has produced an anomaly amplitude of 18.5 milligals. To reduce the amplitude to the 17.5 milligals observed on traverse B1-B1' would require the depth to be about 3.8 kilometres. Hence both profiles C-C' and B1-B1''' indicate that the metasediments probably extend no deeper than four kilometres with a trough of sediments 2.5 km deep in a saddle between the Waterhouse and Rum Jungle Complex.

The gravity high on the profile B1-B1''' at 31 km is due to the sediments in the embayment about 0.7 km from the traverse. The gravity high at 40 km (Plate 4) could be due to a trough of dense basement complex as shown in Model No. 1. The gravity low at 45.5 km is probably due to another wedge of low-density material. Comparison of the geological and gravity maps shows that this low is centred on the boundary of the sediments and complex, so the light material must extend out beneath the sediments.

The discrepancy between the observed and theoretical profiles in the region from 47 to 51 km could be due to dense material (amphi bolite?) in the sediments. An amphibolite body has been located from 47.2 to 47.5 km. However, assuming the body producing the residual anomaly is two-dimensional, of density contrast 0.13 g/cm^3, it would have a cross-section of one square kilometre, which is much larger than the known amphibolite body.

Profile D1-D1': Figure 13 shows the observed and calculated gravity profiles along D1-D1', which crosses the Rum Jungle Complex from northwest to southeast, the embayment, and the Giants Reef Fault. The depth to which the metasediments extend is again about 3 km. The probable width of the low-density material is not constant along the traverse, but it is unlikely that the density contrast for a homogeneous model would extend below 4 km.

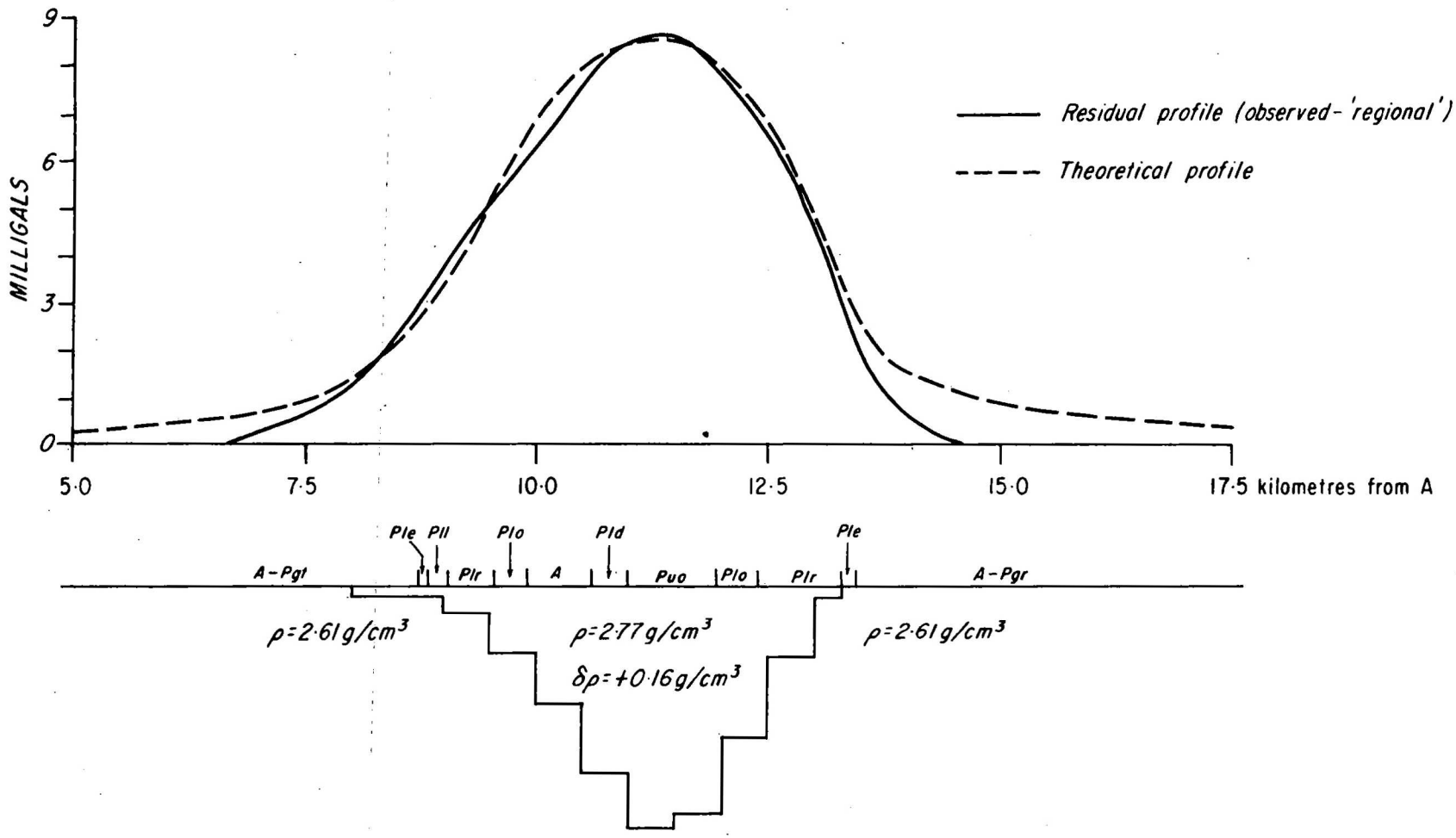

PROFILE A-A' SEDIMENTARY TROUGH BETWEEN
WATERHOUSE AND RUM JUNGLE COMPLEXES

Fig. 12

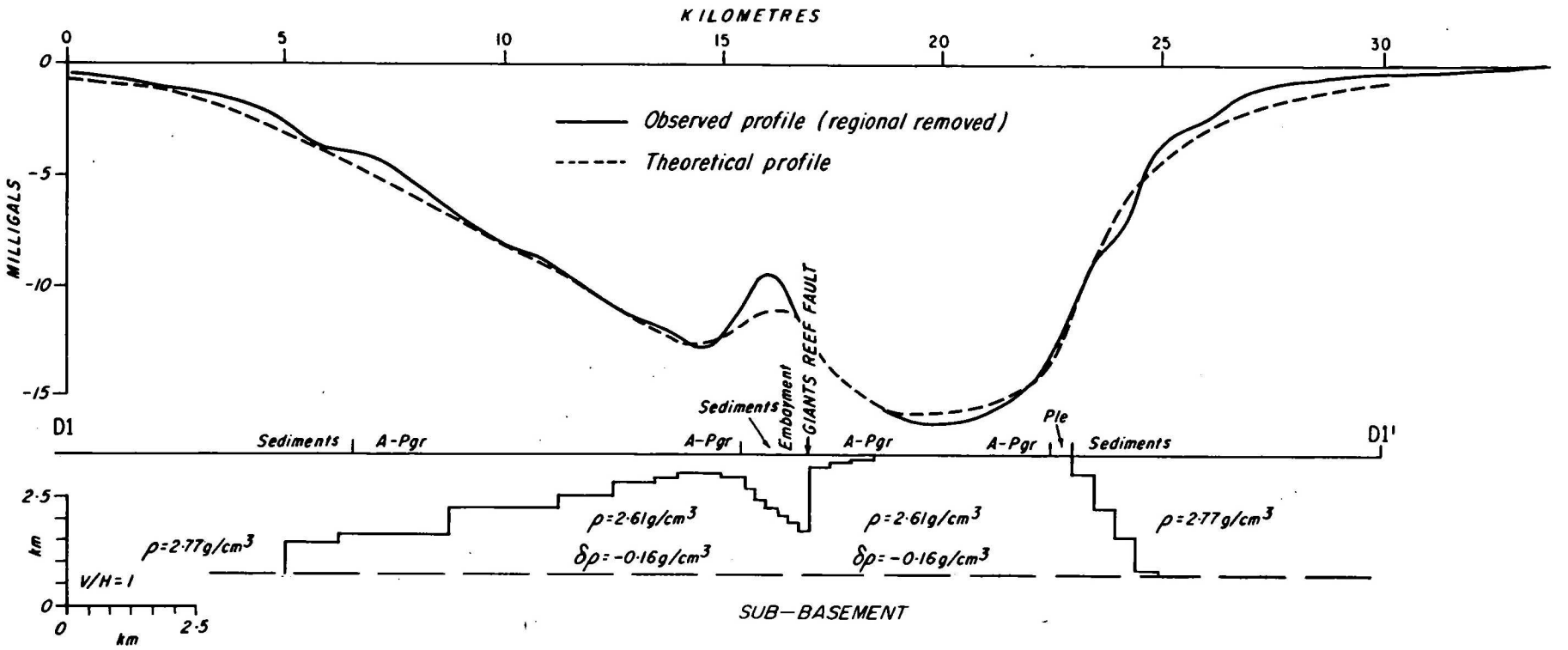

PROFILE DI-DI' RUM JUNGLE COMPLEX

On the southern boundary of the Rum Jungle Complex (23 km) the density discontinuity is shown dipping at 55 degrees. This is consistent with geological dips measured on the Crater Formation in that area.

The low-density material is shown 0.4 km below the surface north of the embayment (15 km). However, the profile fit over the embayment is poor and the light material probably approaches closer to the surface at 14.5 km, where there is a sharp dip in the profile.

Across the embayment the observed profile is much more peaked than the calculated profile. This indicates that the density contrast used in the calculations is too small. If the embayment model is made deeper with the same density contrast then the calculated profile will be wider with only a small increase in amplitude.

9.4 Modelling of Embayment area

Profile U-U': This profile crosses the embayment at almost the same place as profile D1-D1'. Stations were read at 200-m intervals, and their locations are shown beneath the observed profile in Figure 14. The two dashed lines are gradients not associated with the embayment sediments. The lower one corresponds to the main trend of the observed gravity on profile D1-D1' (Fig. 13). If the lower trend is subtracted from the observed profile then the residual profile extends from 1.0 km to 7.5 km. This residual is much broader than the outcrop of sediments, which extends from 3.4 km to 5.2 km, and could not be due to the sediments alone. The flanks of this anomaly extend over the Rum Jungle Complex and may be due to a near-surface increase in the density within the Complex.

The change in slope of the observed profile at 2.5 km is considered to be due to the effects of the sediments in the embayment. Consequently a regional gradient was drawn from this point almost parallel to the lower trend. The residual profile due to the sediments was then obtained by subtracting this regional gradient from the observed profile. Three possible models for the residual anomaly due to the sediments on traverse U-U' are shown in Figure 14.

Fig. 14

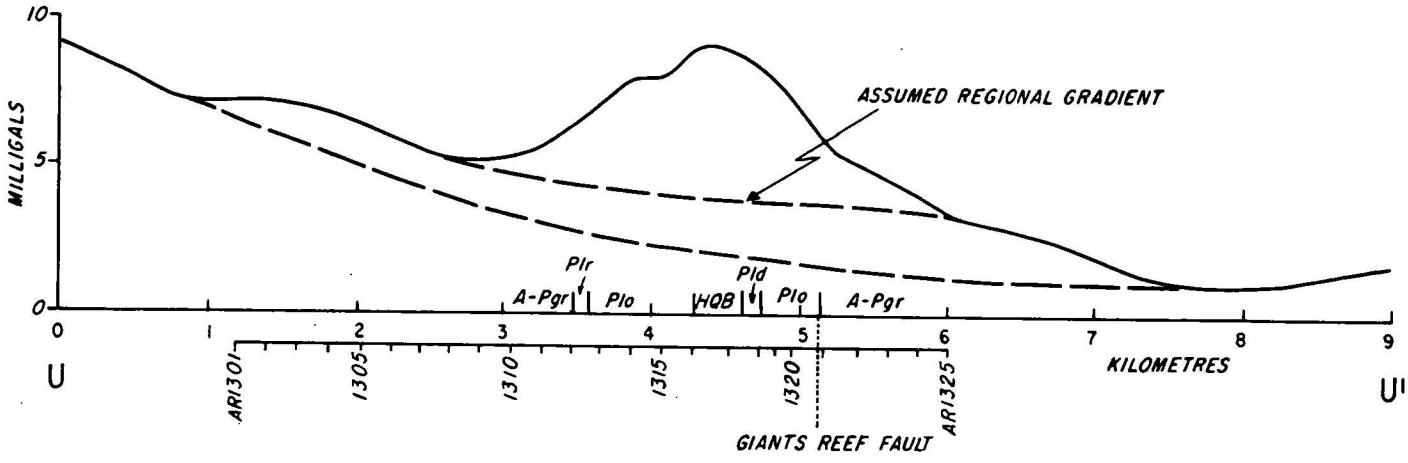

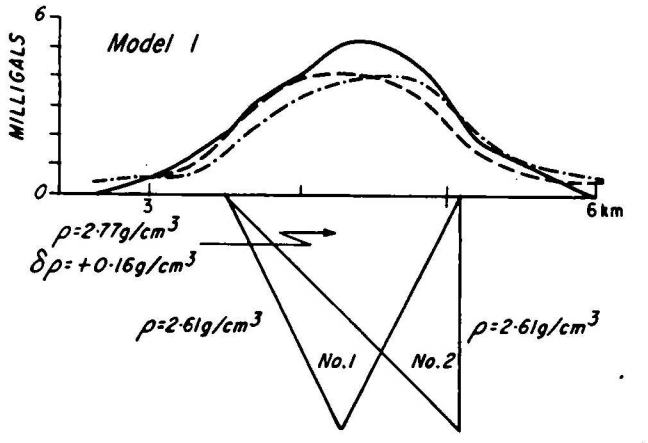

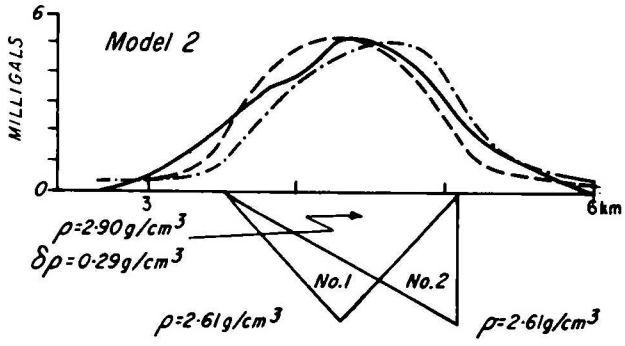

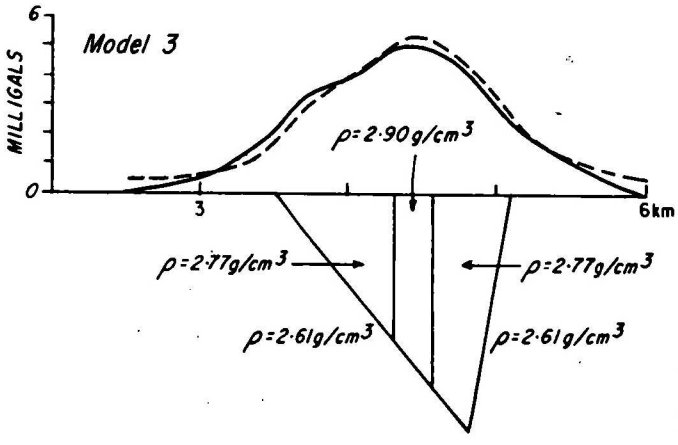

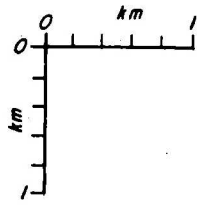

Residual profile

Theoretical profiles

PROFILE U–U' EMBAYMENT AREA

Models 1 and 2 are triangular bodies whose bases coincide with the outcrop of embayment sediments. Model 1 has a density contrast of +0.16 g/cm^3 and model 2 has a density contrast of +0.29 g/cm^3. The depths of the triangular bodies were calculated so that the areas under the theoretical and observed curves are equal. With a density contrast of 0.16 g/cm^3 the depth of the models was 1.6 km and the theoretical profiles are too small in amplitude and too broad. If the dense material (sediment) is extended to greater depth, the anomaly will be broader but without an appreciable increase in amplitude. With a density contrast of 0.29 g/cm^3 the theoretical profiles, although of the correct amplitude, are not a good fit to the observed curve.

Model 3 provides a better fit to the observed residual and assumes a central core of high-density material within a triangular body.

The outcrop of this dense material coincides with outcrop of hematite-quartzite breccia (HQB), but this does not necessarily imply that HQB forms a dense core within the embayment. It could be that the HQB overlies more-dense material, possibly massive dolomite or amphibolite.

Profile V-V': This profile crosses the mouth of the embayment and passes within 0.5 km of Browns prospect. It is in approximately the same position as Daly, Horvath & Tate's (1962) traverse along 9800 west, and the observed profiles agree well.

The approach to modelling on this profile was the same as that used on U-U'. A regional gradient was removed to give a residual profile (Fig. 15). Triangular model 1 with a density contrast of +0.16 g/cm^3 was insufficiently peaked, and to obtain a more peaked curve, model 2 with a uniform density contrast of 0.29 g/cm^3 was proposed. The fit for model 2 is better but the rounded top of the calculated profile does not fit well with the more angular top of the observed profile. The kinks within the observed profile indicate near-surface density variations within the sediment. Model 3 with a core of high-density material provides a better fit to the peak of the curve. The outcrop of this dense material falls mainly in sediment mapped as Coomalie Dolomite. This dense material may represent particularly compact dolomite. The size and mass of these bodies of dense material is far too large for the orebody at Browns to be the source of the peak in the gravity curve.

Record No. 1977/9

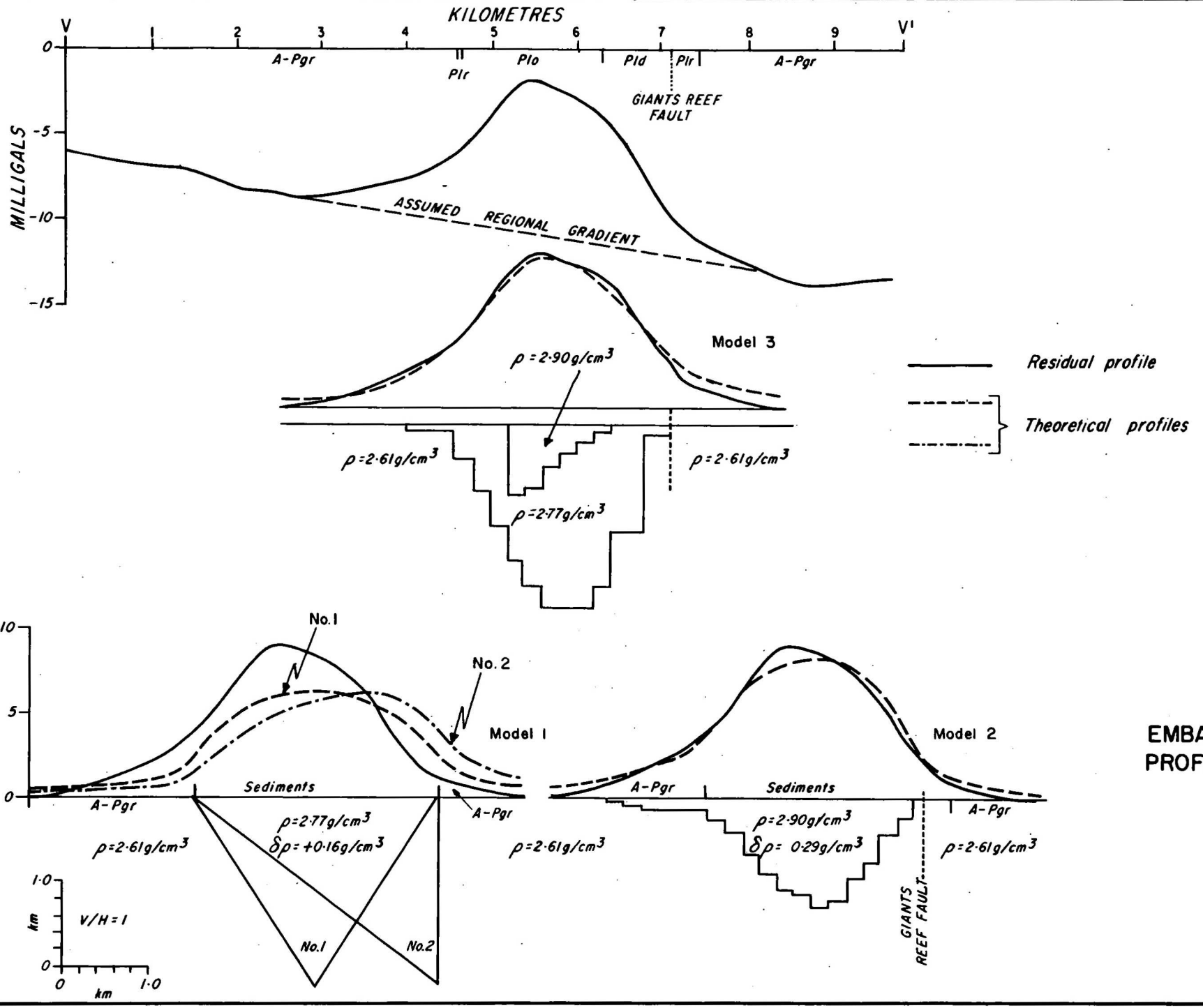

EMBAYMENT
PROFILE V–V'

D52/B7-665A

Fig 15

The embayment appears to extend to a depth of 1.6 km on profile U-U'. Modelling across the mouth of the embayment on profile V-V' indicates a depth of 2.2 km; hence between these profiles the floor of the embayment appears to plunge to the west at about 15 degrees.

9.5 Modelling of Giants Reef Fault

The residual Bouguer anomaly contours shown on Plate 3 show no strong gravity gradient associated with the Giants Reef Fault. This is not surprising when sediment is fault against sediment or complex against complex, but there is also no expression of the Fault on the eastern margin of the Rum Jungle Complex where the fault separates the complex and metasediments. Modelling along profile C1-C1' which crosses the eastern margin of the Rum Jungle Complex indicates that there is no vertical displacement of low or high density rocks across the fault.

Profile C1-C1': Figure 16 shows the observed gravity profile and two-dimensional model along profile C1-C1' which crosses the Giants Reef Fault almost at 90^{o} on the eastern side of the Rum Jungle Complex. The most interesting feature of the profile is the lack of change across the fault from basement complex in the west to sediments in the east. This was the main reason for assuming that the sediments and parts of the basement complexes have the same density. The model shows a density contrast between the low-density complex and the surrounding meta-sediments extending 3.5 km east of the fault at 0.5 km depth. This is necessary to obtain the steep gradient between 16.5 and 18 km.

There is a substantial discrepancy between the modelling of profile C1-C1' and profile B1''-B1''' (Plate 4) which crosses the fault 7 km southwest of profile C1-C'. However, neither model indicates any vertical displacement of rocks across the fault.

9.6 Dips of the contacts

Theoretical curves were plotted over the outcropping contact between a semi-infinite slab of uniform density contrast for various dips of the contact. If Ac denotes the anomaly at the contact and At denotes the total anomaly, then there are simple linear relations between Ac/At and the dip of the contact. These relations are indicated in Figure 17. The first diagram represents a granite

Record No. 1977/9

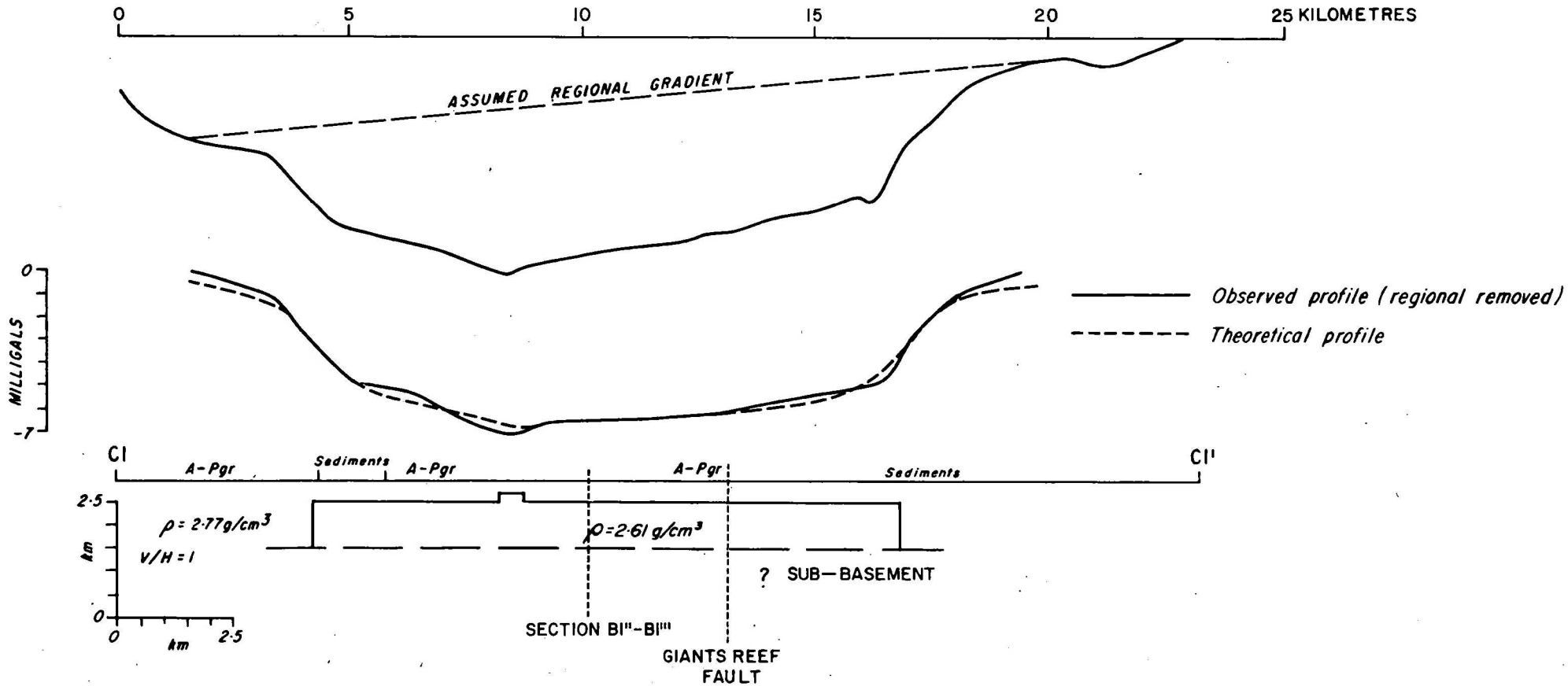

PROFILE C—C1' RUM JUNGLE COMPLEX
AND GIANTS REEF FAULT

D52/B7-666A

Fig 16

Fig. 17

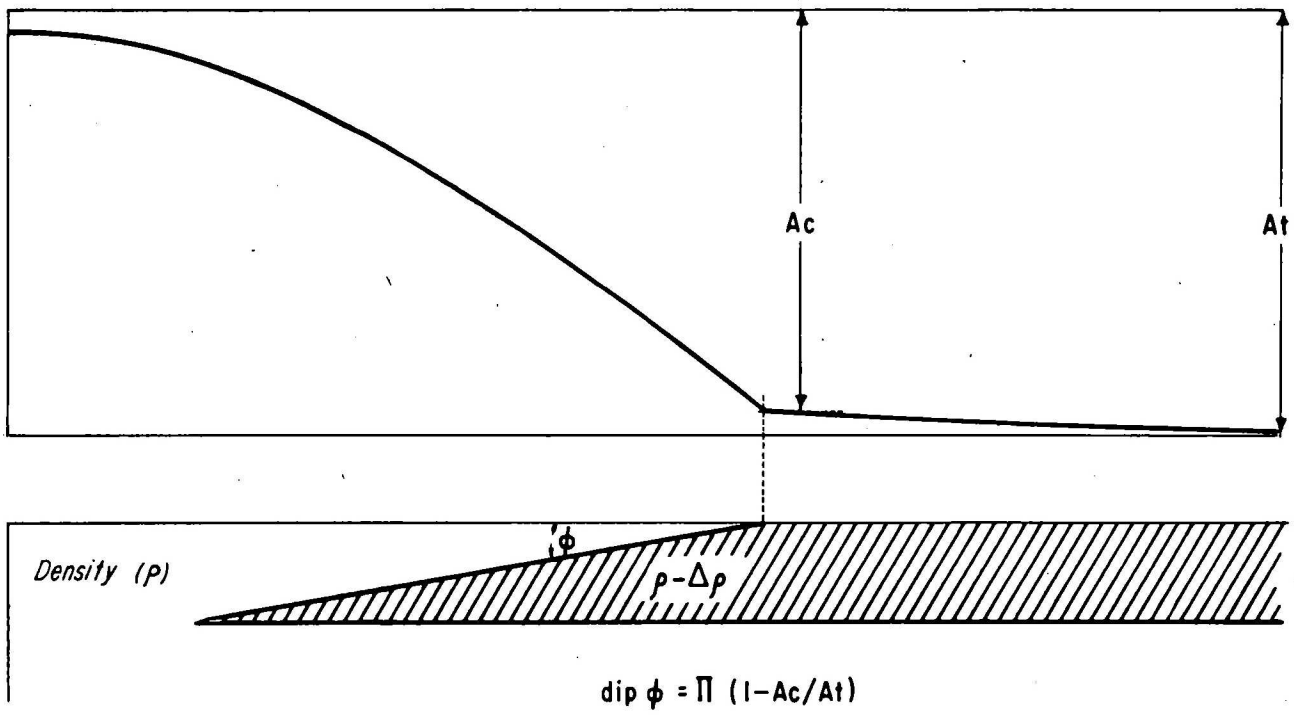

dip $\phi = \Pi\ (1 - Ac/At)$

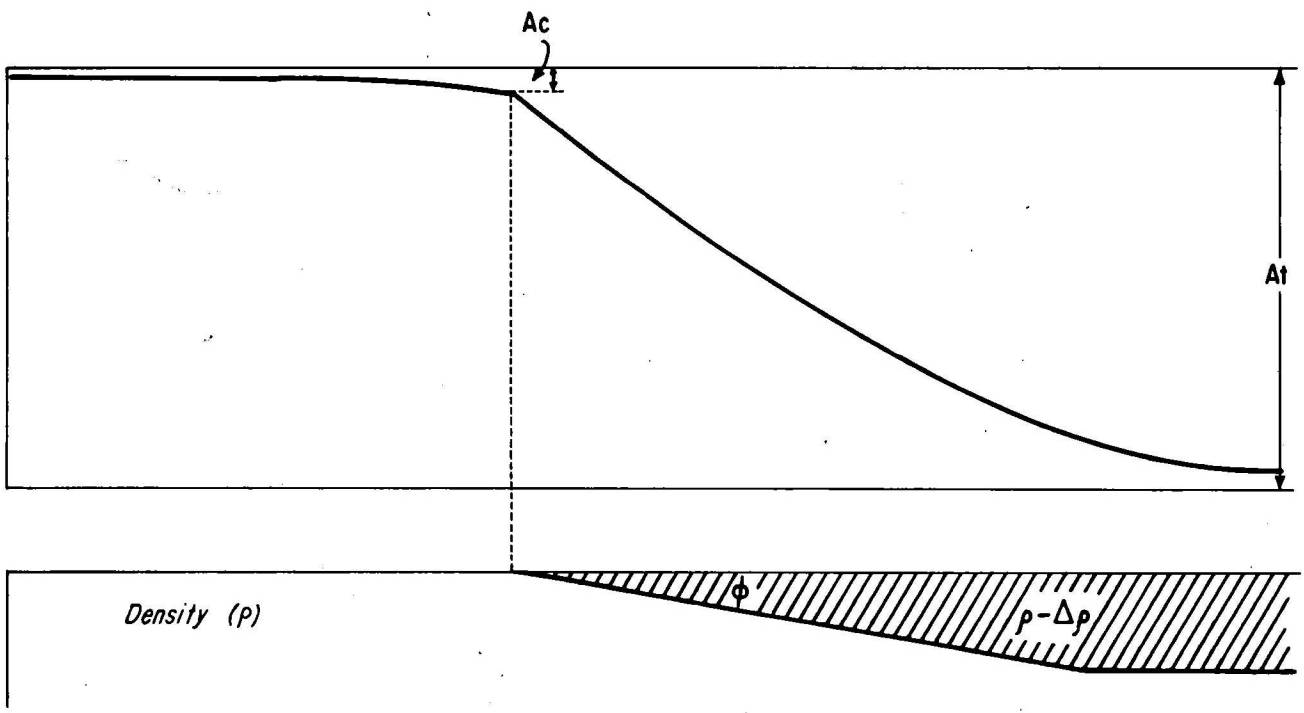

dip $\phi = \Pi\ (Ac/At)$

DIP ESTIMATES FOR OUTCROPPING SLOPING CONTACT

batholith which comprises light material with the contact dipping outward, whereas the second diagram is more representative of a sedimentary basin which comprises light material with the contact dipping inwards.

In practice only rough estimates of the dips can be obtained using these relations. This is because of interference from neighbouring anomalies, uncertainties in density, and uncertainties in the location of the contact. The last factor is the greatest source of error in the dip estimates. Not all of the complexes are of a low density, and hence contacts between the complexes and the sediments are not necessarily the density discontinuities whose dips we wish to estimate. The estimates are generally valid provided the body is broader than it is deep and provided the density contrast is uniform.

Profiles from over the Waterhouse Complex showing dips are given in Plate 5. Figure 18 shows the profiles and dips on the margins of the Rum Jungle Complex. The solid lines represent the dips estimated from the gravity profiles and are denoted E. Geological dips, measured on the sediments at the surface, are shown as a broken line with the symbol G.

All the profiles on the Waterhouse Complex are simple in shape and a reasonable estimate of Ac and At can be obtained. Over the Rum Jungle Complex the method was less successful for three reasons. Firstly, the profiles are more complex and hence it is more difficult to estimate Ac and At. Secondly, the anomalies are smaller and hence they are more easily affected by noise due to surface density variations. Thirdly, the gravity pattern on the Rum Jungle Complex is more complicated than on the Waterhouse Complex. Hence the assumption that the density discontinuity is associated with the complex/sediment contact is less reliable for the Rum Jungle Complex than for the Waterhouse Complex.

Profile B-B' is noisy, but the anomaly amplitude is large and the dip can be reliably estimated.

Record No. 1977/9

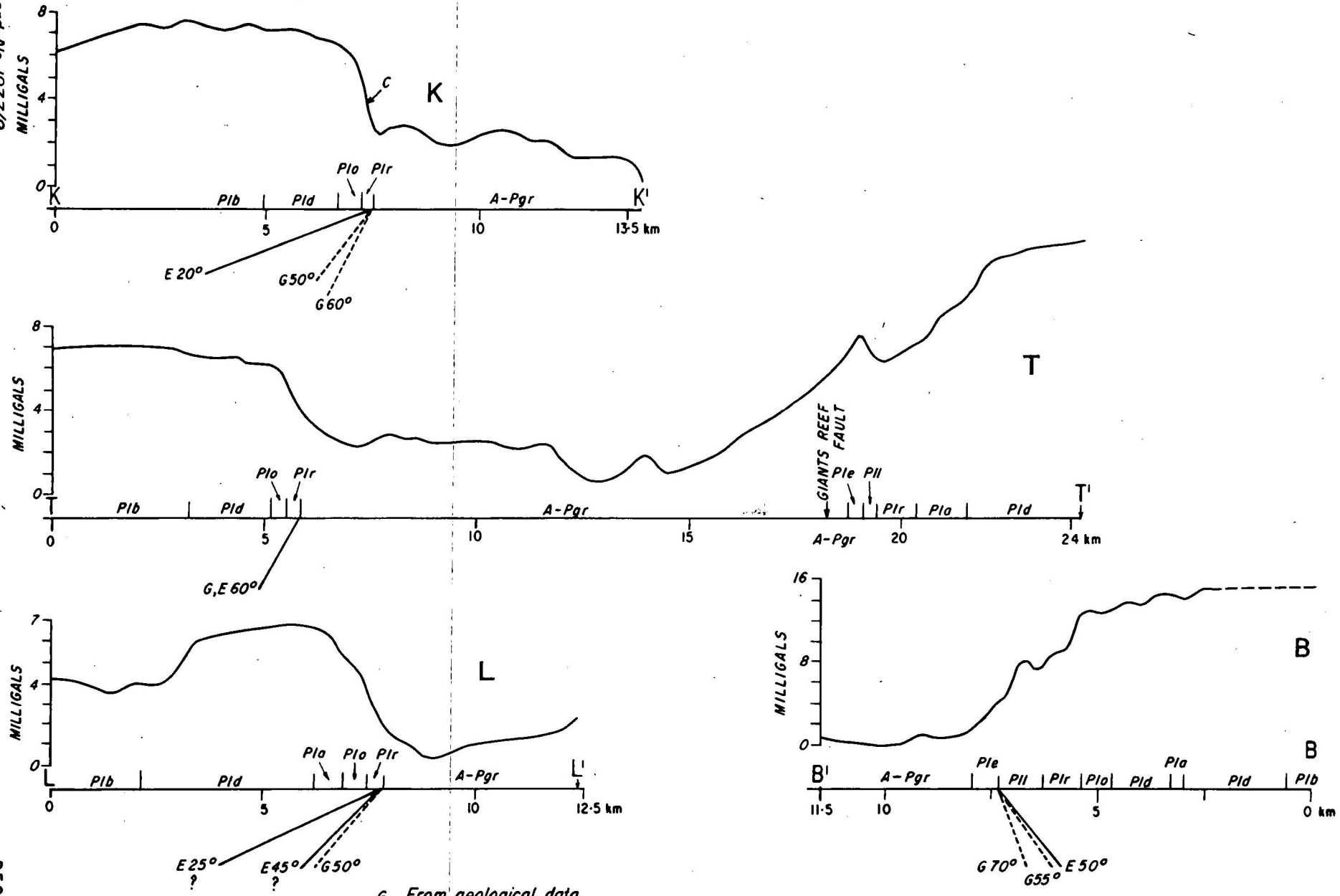

G From geological data

E From gravity data

DIP ESTIMATES AROUND THE RUM JUNGLE COMPLEX

Fig 18

D52/B7-669A

Profile T-T' is taken along line 120 south described by Gardener (1971a). The dip obtained on the western margin of the complex was 60^{o}, which agrees with geological dips in the area and Gardener's estimate of 70^{o}. At the eastern margin the profile is complicated and a good estimate of Ac and At cannot be obtained.

On profiles K-K' and L-L' the anomalies near the contact are simple and well-defined; however, the estimated and geological dips do not agree well. The dip estimate of 20^{o} on K-K' is probably incorrect because surface geological dips are 50^{o} to 60^{o}. Also on profile T-T', one kilometre south, the estimated dip is 60^{o}. Since there is no appreciable change in the width of the Coomalie Dolomite outcrop between traverses K-K' and T-T' there is no geological evidence for a change from 60^{o} to 20^{o}. On profile K-K' the estimated dip is too sensitive to variations in the contact position. If the contact is moved only 150 m to the point C then the method gives a dip of 60^{o}. Another reason for favouring a dip steeper than 20^{o} is the shape of the profile, which approximates the symmetrical profile for a 90^{o} dip rather than the asymmetrical profile for a 20^{o} dip.

On profile L-L' a local gravity high between 3.5 and 6.5 km obscures the top of the anomaly. This, in turn, makes a dip estimate on this profile unreliable. By keeping the contact fixed and making different estimates on the maximum and minimum anomaly, dip angles ranging from 25^{o} to 45^{o} were obtained.

9.7 Calculations of deficient mass

The deficient mass can be uniquely determined from the gravity anomaly without making any assumptions about the densities of the bodies involved. The calculations are in Appendix 5. For both the Rum Jungle and Waterhouse Complexes the total deficient mass was 1.5×10^{17} g.

If we assume that the deficient mass is due to a body of density contrast -0.16 g/cm^3 the volume of this body would be 940 km^3. The surface areas of the Rum Jungle Complex and Waterhouse Complex are 228 km^2 and 112 km^2 respectively which give a total area of 340 km^2. If we further assume all this area is underlain by material of density

contrast -0.16 g/cm^3, distributed in the form of vertical cylinders, then the depth of the cylinders (or the depth of the metasediments) is 2.8 km. But if the dips of the contacts are outwards, so that the cross-sectional area of the low-density material increases with depth, then the depth extent of the sediments would be less than 2.8 km. This is inconsistent with the figure of 3.8 km obtained from the profiles.

A feasible explanation for the discrepancy between the model based on deficient mass calculations and those based on modelling is that not all of the complexes are underlain by low-density material. If we suppose that only those parts of the Rum Jungle Complex associated with strong gravity anomalies are underlain by low-density material, then the surface area of low-density rocks is about 100 km^2. This, added to the area of the Waterhouse Complex, gives a total area of 212 km^2. Assuming a cylindrical density distribution, this would imply that the sediments have a depth of 4.4 km. If the low-density material broadens with depth then the density contrast would extend to less than 4.4 km. This is consistent with the other modelling, which gave a depth of about 4 km.

10. CONCLUSIONS

The gravity method cannot be used to map the complex/sediment contact everywhere because parts of the complexes have the same density as the surrounding sediments. However, in most areas there is a density contrast between the complexes and the metasediments, and in these areas the geometry of the low-density parts of the complexes can be estimated. The low-density parts of the Rum Jungle Complex can be roughly correlated with the leucocratic granite described by Rhodes (1965). The low-density parts of both the Rum Jungle Complex and Waterhouse Complex may represent a diapiric granite as postulated by Stephansson & Johnson (1975). Two-dimensional models, corrected for end effects, suggest that the thickness of metasediments in the Rum Jungle area is less than 4 km and that the sediments in the saddle between the Rum Jungle Complex and Waterhouse Complex are less than 3 km deep. The similarity in density between the metasediments and parts of the basement complexes might imply a similar geological history for these two rock types and might further support Stephannsson & Johnson's (1975) postulates regarding diapirism.

The sediments in the embayment deepen to the west and contain dense material which is probably amphibolite or massive dolomite. Features of the gravity profiles across the embayment cannot be explained by known mineral deposits (e.g. Browns prospect), which are too small to produce the observed anomalies.

Dip estimates of the complex/sediment contact agree in some areas with observed surface geological dips measured in the sediments, but in other areas the estimated and geological dips disagree. A large source of error in estimating dips from the gravity profiles is the uncertainty in the surface positions of the density discontinuity whose dip we seek.

Although the mass deficiency of the complexes can be uniquely determined, the models represent only one possible distribution of this mass. If we assume a value for the density contrast then the deficient mass can be used to calculate the volume of material producing the anomaly.

Two-dimensional modelling with end corrections is limited and possibly gives unrealistic results when applied to such markedly three-dimensional features as the northern gravity low on the Rum Jungle Complex. Three-dimensional modelling is obviously preferable but is more time consuming because there are more variables. If we consider the uncertainties in the density contrasts and the surface positions of the density discontinuities, the extra effort in making three-dimensional models of the complexes is not justified. Even if a perfect fit to the contours was obtained, the model would be only one density distribution out of many whose gravitational field matches the observed field.

The gravity method is unsuitable for mapping the boundary between the Coomalie Dolomite and the Golden Dyke Formation because there is no consistent density contrast between the two formations and the dolomite outcrops are sometimes associated with gravity lows.

11. REFERENCES

BEATTIE, R.D., 1971 - Airborne gamma-ray spectrometer survey, Rum Jungle, N.T., 1969. Bur. Miner. Resour. Aust. Rec. 1971/85.

BOTT, M.H.P., 1956 - A geophysical study of the granite problem. Geol. Soc. London Quart. J., 112, p. 45-67.

BOTT, M.H.P. & SMITH, R.A., 1958 - The estimation of the limiting depth of gravitating bodies. Geophys. Prosp., 6(1), p. 1-10.

BROWNE-COOPER, P.J. & GERDES, R.A., 1970 - Rum Jungle detailed aeromagnetic survey, Northern Territory, 1967. Bur. Miner. Resour. Aust Rec. 1970/111.

BRYAN, R., 1962 - Lower Proterozoic basic intrusive rocks of the Katherine-Darwin area, Northern Territory. Bur. Miner. Resour. Aust. Rec 1962/7.

CLARK, D., 1953 - Plane and geodetic surveying for engineers, vol. 2: Higher surveying, 4th ed. London, Constable.

DALY, J., 1957 - Notes on the results of aeromagnetic surveys in the Northern Territory. Bur. Miner. Resour. Aust. Rec. 1957/72.

DALY, J., HORVATH, J. & TATE, K.H., 1962 - Browns deposit geophysical survey, Rum Jungle, N.T., 1957 Ibid., 1962/146.

DALY, J., & TATE, K.H., 1960 - Waterhouse Nos. 2, 3 and 4 uranium prospects, geophysical surveys, N.T. 1957. Ibid., 1960/109.

DODSON, R.G., & SHATWELL, D.O., 1965 - Geochemical and radiometric survey, Rum Jungle, N.T. 1964. Bur. Miner. Resour. Aust. Rec. 1965/254.

DUCKWORTH, K., FARROW, B.B., & GARDENER, J.E.F., 1968 - Rum Jungle East test geophysical surveys, Northern Territory, 1966-1967. Bur. Miner. Resour. Aust. Rec. 1968/45.

GARDENER, J.E.F., 1971a - Geophysical surveys of the Rum Jungle Complex, Northern Territory, 1968. Ibid., 1971/20.

GARDENER, J.E.F., 1971b - Manton area reconnaissance geophysical survey, N.T., 1968. Ibid., 1971/23.

GRANT, F.S. & WEST, G.F., 1965 - Interpretation theory in applied geophysics. New York, McGraw-Hill.

JOHNSON, K., 1974 - Progress report: geological review and revision of the Rum Jungle area, Northern Territory, 1973. Bur. Miner. Resour. Aust. Rec. 1974/41.

LANGRON, W.J., 1956 - Geophysical survey in the Rum Jungle area, N.T., 1954. Ibid.,-1956/43.

OGILVY, R.D., in prep. - Rum Jungle area geophysical survey, Northern Territory, 1974. Bur. Miner. Resour. Aust. Rec.

RHODES, J.M., 1965 - The geological relationships of the Rum Jungle Complex, Northern Territory. Bur. Miner. Resour. Aust. Rep. 89.

STEPHANSSON, O. & JOHNSON, K., 1975 - Granite diapirism in the Rum Jungle area, Northern Australia. Bur. Miner. Resour. Aust. Rec. 1975/12.

STOTT, P.M., & LANGRON, W.J., 1959 - Report of a reconnaissance gravity survey in the Darwin-Katherine area, Northern Territory, 1955-1957. Ibid., 1959/72.

WALPOLE, B.P., CROHN, P.W., DUNN, P.R. & RANDAL, M.A., 1968 - Geology of the Katherine-Darwin region, Northern Territory. Bur. Miner Resour. Aust. Bull. 82.

WHITWORTH, R., 1970 - Reconnaissance gravity survey of parts of Northern Territory and Western Australia, 1967. Bur. Miner. Resour. Aust. Rec. 1970/15.

WILLIAMS, P.F., 1963 - Geology of the Rum Jungle district, Northern Territory. Territory Enterprises Pty Ltd Report. (unpubl.)

WILLIAMS, J.P., 1970 - Geophysical investigation of the eastern margin of the Rum Jungle Complex, N.T., 1967. Bur. Miner. Resour. Aust Rec. 1970/1.

APPENDIX 1

DENSITY AND SUSCEPTIBILITY MEASUREMENTS ON DRILL CORE

FROM THE 1973 AND 1974 DRILLING AT RUM JUNGLE

Hole number (field)	Hole number (Systematic)	Core store index no.	Laboratory Sample no.	Depth of Hole (metres)	Depth of Sample (metres)	Dry density (g/cm^3)	Polumerric magnetic Susceptibility SI x 10^{-4}	Formation	DESCRIPTION
R8/73	RJ8	2184	75/66	37.5	32.7	2.58	NM	A-Pgr	Granodiorite, leucocratic; mainly quartz & feldspar
R2/74	RJ18	2280	75/73	26.2	26.2	2.70	NM	A-Pgt	Gneissic leucocratic granite biotite-rich layers
R16/74	RJ32	2294	75/90	24.1	23.5	2.63	NM	A-Pgt	Granite gneiss
R28/74	RJ44	2306	75/101	16.8	15.1	2.63	NM	A-Pgt	Biotite-rich prophyritic granite or adamellite
R41/74	RJ55	2319	75/109	21.0	18.0	2.64	NM	A-Pgt	Altered granite, quratz & chlorite, monor pink feldspar
			75/110	21.0	19.7	2.63	NM	A-Pgt	as above
			75/111	21.0	20.9	2.58	NM	A-Pgt	Coarser-grained pegmatitic feldspar rich with chlorite
R9/73	RJ9	2185	75/67	21.3	16.8	2.61	NM	Ple	Recrystallized sandstone, weakly feldspathic

Hole number (field)	Hole number (Systematic)	Core store index no.	Laboratory Sample no.	Depth of Hole (metres)	Depth of Sample (metres)	Dry density (g/cm^3)	Polumerric magnetic Susceptibility SI x 10^{-4}	Formation	DESCRIPTION
R10/73	RJ10	2186	75/68	25.6	21.9	2.57	NM	Ple	Bedded quartz sandstone, some chloritization
R52/74	RJ68	2330	75/123	6.1	5.0	2.54	NM	Ple	Fine-grained bedded sandstone
R54/74	RJ70	2332	75/125	20.0	19.2	2.65	1.3	Ple	Quartz hematite breccia
R16/74	RJ32	2294	75/89	24.1	18.4	2.71	NM	Ple	Chloritized sheared quartzite blebs of pyrite
R51/74	RJ67	2329	75/121	60.7	33.2	2.65	1.0	Ple	Schistose micaceous dolomitic weathered sandstone
			75/122	60.7	60.4	2.13 (2.29) wet	NM	Ple	Quartz sandstone, minor dolomite
R15/73	RJ15	2191	75/70	25.0	24.8	2.97	7.5	P11	Amphibolite with minor pyrite
R16/73	RJ16	2192	75/71	25.0	23.5	2.85	5.0	P11	Amphibolitized calcareous siltstone
			75/72	25.0	24.8	2.76	6.3	P11	as above

Hole number (field)	Hole number (Systematic)	Core store index no.	Laboratory Sample no.	Depth of Hole (metres)	Depth of Sample (metres)	Dry density (g/cm^3)	Polumerric magnetic Susceptibility SI x 10^{-4}	Formation	DESCRIPTION
R3/74	RJ19	2281	75/74	36.6	27.4	2.85	8.8	P11	Indurated amphibolite disseminated pyrrhotite
			75/75	36.6	34.3	2.91	10	P11	Massive amphibolite
R5/74	RJ21	2283	75/77	26.2	22.4	2.91	6.3	P11	Massive well-indurated amphibolite
R14/74	RJ30	2292	75/85	25.3	24.9	2.77	3.8	P11	Calcareous amphibolite with pyrite & chlorite
R15/74	RJ31	2293	75/86	23.8	8.8	2.65	NM	P11	Quartz sandstone, siliceous matrix with muscovite
			75/87	23.8	16.2	2.69	NM	P11	Fine-grained sandstone
			75/88	23.8	23.0	2.66	NM	P11	Feldspathic sandstone, oxidized pyrite disseminated throughout
R17/74	RJ33	2295	75/91	46.3	29.4	2.76	3.8	P11	Chloritic dolomitic amphibolite, pyrite along fracture planes
			75/92	46.3	29.7	2.87	6.3	P11	as above
			75/93	46.3	46.2	2.93	7.5	P11	as above
R53/74	RJ69	2331	75/124	49.4	48.0	2.78	NM	P11	Green dolomite

Hole number (field)	Hole number (Systematic)	Core store index no.	Laboratory Sample no.	Depth of Hole (metres)	Depth of Sample (metres)	Dry density (g/cm^3)	Polumerric magnetic Susceptibility SI x 10^{-4}	Formation	DESCRIPTION
R37/74	RJ53	2315	75/105	42.1	36.1	2.76	5.0	Plr	Well-foliated silty shale
R6/73	RJ6	2182	75/64	29.6	26.5	2.98	NM	Plo	Dolomitic marble
			75/65	29.6	28.0	2.95	NM	Plo	Dolomite with minor talc
R14/73	RJ14	2190	75/69	35.4	34.9	2.99	NM	Plo	Dolomite
R4/74	RJ20	2282	75/76	32.3	30.5	2.70	NM	Plo	Quartz & chert breccia in hematite matrix
R6/74	RJ22	2284	75/78	117.7	117.7	2.86	NM	Plo	Crystalline carbonate with minor hematite
R8/74	RJ24	2286	75/80	50.9	50.7	2.78	NM	Plo	Dolomite with chlorite
R24/74	RJ40	2302	75/96	18.3	10.1	2.63	NM	Plo	Marble enclosed within quartzite
			75/97	18.3	17.5	2.84	NM	Plo	Dolomite
R25/74	RJ41	2303	75/98	16.5	15.5	2.78	0.5	Plo	Tremolitic dolomite, minor pyrite & pyrrhotite
R26/74	RJ42	2304	75/99	20.4	12.3	2.81	1.0	Plo	Fine-grained dolomite & amphibolite
			75/100	20.4	14.0	2.80	0.9	Plo	Dolomite

Hole number (field)	Hole number (Systematic)	Core store index no.	Laboratory Sample no.	Depth of Hole (metres)	Depth of Sample (metres)	Dry density (g/cm^3)	Polumerric magnetic Susceptibility SI x 10^{-4}	Formation	DESCRIPTION
R30/74	RJ46	2308	75/102	34.1	33.6	2.88	NM	Plo	Coarsely crystalline dolomite
R32/74	RJ48	2310	75/103	12.2	9.3	2.81	NM	Plo	Dolomitic marble
R35/74	RJ51	2313	75/104	37.8	36.0	3.00	10	Plo	Calcareous amphibolite
R38/74	RJ54	2316	75/106	30.8	30.8	3.01	10	Plo	Dense foliated non-calcareous amphibolite
R40/74	RJ56	2318	75/108	15.8	15.7	2.41	NM	Plo	Quartzite (silicified carbonate) not fresh
R42/74	RJ58	2320	75/112	15.2	15.1	2.96	NM	Plo	Dolomitic marble
R43/74	RJ59	2321	75/113	43.9	43.9	2.98	NM	Plo	Dolomite with chlorite
R44/74	RJ60	2322	75/114	16.5	16.3	2.83	NM	Plo	Siliceous dolomite with minor pyrite
R45/74	RJ61	2323	75/115	24.4	24.1	2.82	0.6	Plo	Shaly dolomite containing weathered sulphides
R46/74	RJ62	2324	75/116	46.6	46.5	2.76	NM	Plo	Dolomite
R47/74	RJ63	2325	75/117	26.0	26.0	2.77	NM	Plo	Dolomite
R48/74	RJ64	2326	75/118	26.8	27.4	2.86	NM	Plo	Dolomite
R49/74	RJ65	2327	75/119	14.9	14.0	2.82	5.0	Plo/ Pld	Calcareous amphibolite

Hole number (field)	Hole number (Systematic)	Core store index no.	Laboratory Sample no.	Depth of Hole (metres)	Depth of Sample (metres)	Dry density (g/cm^3)	Polumerric magnetic Susceptibility SI x 10^{-4}	Formation	DESCRIPTION
R50/74	RJ66	2328	75/120	9.8	9.6	2.98	7.5	Plo/ Pld	Calcareous amphibolite minor disseminated sulphides
R57/74	RJ73	2335	75/127	10.7	10.4	2.95	NM	Plo	Dolomitic marble
R1/73	RJ1	2177	75/60	36.3	36.3	2.90	7.5	Pld	Amphibolite
R3/73	RJ3	2179	75/61	66.1	43.1	2.75	3.8	Pld	Calcareous siltstone
R4/73	RJ4	2180	75/62	31.4	24.5	2.78	2.5	Pld	Calcareous black shale with pyrite
R5/73	RJ5	2181	75/63	53.3	52.4	2.80	0.7	Pld	Calcareous black shale with pyrite & graphite
R7/74	RJ23	2285	75/79	17.1	16.2	2.97	7.5	Pld	Massive and well-indurated amphibolite
R9/74	RJ25	2287	75/81	29.9	28.0	2.31	2.5	Pld	Black calcareous pyritic shale
R11/74	RJ27	2289	75/82	33.8	32.9	2.95	10	Pld	Calcareous amphibolite, minor chlorite & sulphide
R12/74	RJ28	2290	75/83	54.9	54.8	2.57	2.5	Pld	Black calcareous pyritic shale
R13/74	RJ29	2291	75/84	47.2	46.9	2.51	2.5	Pld	Black calcareous pyritic shale
R23/74	RJ39	2301	75/94	52.4	44.3	2.84	NM	Pld?	Dolomite

Hole number (field)	Hole number (Systematic)	Core store index no.	Laboratory Sample no.	Depth of Hole (metres)	Depth of Sample (metres)	Dry density (g/cm^3)	Polumerric magnetic Susceptibility SI x 10^{-4}	Formation	DESCRIPTION
			75/95	52.4	51.9	2.75	NM	P1d?	Dolomitic shale
R39/74	RJ55	2317	75/107	22.6	21.8	2.47	6.3	P1b	Phyllitic siltstone
R56/74	RJ72	2334	75/126	6.4	6.2	2.55	NM	Puo	Quartzite

NM denotes no measurement.

APPENDIX 2
EQUIPMENT

Characteristics of the three Worden gravity meters used in the survey are tabulated below.

METER	CALIBRATION FACTOR Milligal/Div.	DATES OF USE	COMMENTS
W260	0.1088	14/05 to 13/08	Drift slightly high, probably needs re-evacuation.
W140	0.1019(8)	14/05 to 26/06	Drift satisfactory, optical system failed on 26/06.
W 61	0.090303	10/07 to 19/09	Limited range meter. Tendency to jump 0.5 dial divisions one or two minutes after first reading.

For levelling the detailed traverses BMR personnel used a Topcon automatic level model AT-32 on loan from the Division of National Mapping.

For barometric levelling several Mechanism Ltd precision aneroid microbarometers type M2236/A were used. Serial numbers 260, 261, and 263 formed the mobile bank and numbers 294, 264, and 317 formed the base bank. On the 19/07/74, number 294 gave inconsistent readings and was replaced by number 529.

APPENDIX 3

STATION IDENTIFICATION

Most stations were marked with wooden stakes about 0.5 m high bearing an identifying number. Levels and gravity readings were taken on a small star picket driven in flush to the ground surface. Every fifth spirit levelled station was made 'permanent' by marking it with a steel star picket about one metre high. At these stations the small star picket was set in concrete. In the field the stations were identified by two letters followed by a number, e.g., AD 7.5, denoting that this station was approximately 7.5 kilometres along traverse AD.

For field station AD 7.5 the BMR station number is 7408.0515. On the gravity map the 7408 is replaced by the symbol AB, hence the station appears as AB0515. Every fifth station is labelled on the gravity map but these stations do not necessarily coincide with the 'permanent' field stations. In the symbol 7408.0515, the 74 is the year of the survey, the 08 is the identifier for the Rum Jungle gravity survey, the 05 is the traverse identifier and the 15 identifies the fifteenth station (which is 7.5 on this traverse). The table below shows the relation between the alphabetic traverse identifier used in the field and the numeric traverse identified used on the gravity map.

TABLE FOR APPENDIX 3

alphabetic name	levelling method	numeric name	alphabetic name	levelling method	numeric name	alphabetic name	levelling method	numeric name	alphabetic name	levelling method	numeric name	alphabetic name	levelling method	numeric
AA (N)	S	01	Ba	S	21	CA	B	39	EA	B	62	DETAIL		
AA (S)	S	02	BB	S/B	22	CB	B	40	EB	B	63	No.1	S	77
AB	S	03	BC	S	23	CC	B	41	EC	B	64	No.2	S	78
AC	S	04	BD	S	24	CD	B	42				No.3	S	79

alphabetic name	levelling method	numeric name	alphabetic name	levelling method	numeric name	alphabetic name	levelling method	numeric name	alphabetic name	levelling method	numeric name	alphabetic name	levelling method	numeric name
AD	S	05	BE	S	25	CE	B	43	FA	B	65	No.4	S	80
AG	S	06	XY	S	25	CF	B	44	FB	S	66	No.5	S	81
AH	S	07	XZ	S	25	CG	S	45	FC	B	67	No.6	S	82
AI	S	08	BF	S/B	26	CH	B	46	FD	B	68	No.7	S	83
AJ	S	09	BG	S	27	CI	B	47	FE	B	69	No.8	S	84
AL	S	10	BH	S	28	CJ	S	48	FF	B	70	No.11	S	85
AM	S	11	BI	S	29	CK	S	49	FG	B	71	No.12	S	86
AN	S	12	BJ	S	30	CL	B	50	FH	B	72	No.13	S	87
AO	S	13	BK	S	31	CM	B	51	FI	B	73	No.14	S	88
AP	S	14	BL	B	32	CN	B	52				No.17	S	89
AQ	S	15	BO	S	33	CO	S	53	NA	S/B	74			
AR(N)	S	16	BP	S	34	CP	B	54						
AR(S)	S	17	BR	S	35	CQ	B	55	WATER-HOUSE					
AS	S	18	BS	S	36	CR	B	56	WEST	S	75			
AW	S	19	BT	S	37	CS	B	57	EAST	S	76			
AZ	S	20	BV	S	38	CT	B	58						
						CV	B	59						
						CW	B	60						
						CZ	B	61						

S - DENOTES SPIRIT LEVELLED TRAVERSE

B - DENOTES BAROMETRICALLY LEVELLED TRAVERSE

(N) denotes northerly traverse

(S) denotes southerly traverse

APPENDIX 4

BAROMETRIC LEVELLING FORMULA AND ERRORS

The formula for reducing the barometric readings to height differences is based on a modification of the formula given by Clark (1953). The simplified formula is

$$h = hs - hb = 67.4021\ T \log_{10}\left(\frac{Pb}{Ps}\right) \quad \text{metres}$$

where
- h is the height difference (metres)
- hs is the height of the station (metres)
- hb is the height of the base (metres)
- T is the mean temperature of the air column (Kelvin)
- Pb is the pressure reading at the base) arbitrary
- Ps is the pressure reading at the station) units

To examine the dependence of height errors on temperature errors we differentiate with respect to T

$$\frac{dh}{dT} = 67.4021 \log_{10}\left(\frac{Pb}{Ps}\right) = \frac{h}{T}$$

if h = 50 m
and T = 300°K

$$\frac{dh}{dT} = \frac{1}{6}$$

hence

$$\delta h = 17\ \delta T \quad \text{cm.}$$

Hence, for a height difference of 50 m, the height error would be 17 cm per degree Celcius. To examine the dependence of height errors on pressure errors we differentiate with respect to Pb.

$$h = 67.4021\ T\ \log_{10}e.\ \ln\left(\frac{Pb}{Ps}\right)$$

$$= 29.27236\ T\ (\ln Pb - \ln Ps) \qquad \text{metres}$$

$$\frac{dh}{dPb} = \frac{29.27236\ T}{Pb}$$

now if $T = 300^{o}K$

and $Pb = 1000$ mb

$$\frac{dh}{dPb} = 8.8$$

hence $\delta h = 8.8\ \delta Pb$ metres

The pressure can be estimated with an error of $\pm$ 0.01 millibar on the Mechanism barometers and this error corresponds to a height difference of $\pm$ 9 cm.

APPENDIX 5
CALCULATION OF DEFICIENT MASS

The deficient mass of a three-dimensional body producing a gravity anomaly can be calculated from the formula (Grant & West, 1965, p. 228)

$$\int_{-\infty}^{\infty}\int_{-\infty}^{\infty} \Delta g\,(x, y)\ dx\ dy = 2\pi G M$$

where G is the gravitational constant (6.67×10^{-8} c.g.s. units)

M is the mass deficit (g)

$\Delta g\,(x, y)$ is the gravity anomaly in the x, y plane.

This formula involves no assumptions about the density contrast of the body. The formula requires a double integration over the x, y plane from $-\infty$ to ∞. Obviously the anomaly can be traced only a finite distance from its source before it decays into the background noise. Hence in practice we can only integrate the anomaly over a finite range of x and y. If we denote this integration over a finite range by

$$I = \int_{-X}^{X}\int_{-Y}^{Y} \Delta g\,(x, y)\ dx\ dy$$

then the deficient mass is related to this integral by the formula (Grant & West, 1965, p. 270)

$$M \simeq \frac{I}{4G}\left(\operatorname{artan}\frac{XY}{zR}\right)^{-1}$$

where G and M have the same meanings as before

X is the x range of integration

Y is the y range of integration

$R = \sqrt{(X^2 + Y^2)}$

$\bar{z}$ is the depth of the centre of mass of the body.

To evaluate I, nineteen east-west profiles 2.5 km apart were drawn across the anomaly. Along each profile about 25 points were selected one kilometre apart and the anomaly value from the contour map was read at each point.

Integration with respect to x was performed using Simpson's rule along each profile. Simpson's rule was again used to integrate with respect to y and the result obtained was $I = 5.526 \times 10^{10}$ gal-cm^2

hence $2\pi G M \simeq 5.526 \times 10^{10}$

and $M = 1.3 \times 10^{17}$ g.

If we want to allow for the finite range of integration then we put

$$\left.\begin{aligned} X &= 11 \text{ km} \\ Y &= 20 \text{ km} \end{aligned}\right\} \quad R = 22.8 \text{ km}$$

$$\overline{z} = 2 \text{ km}$$

in the formula and obtain

$$M = \frac{5.526 \times 10^{10}}{4 \times 6.67 \times 10^{-8}} \left(\arctan \frac{11 \times 20}{2 \times 22.8} \right) - 1$$

$$= 1.5 \times 10^{17} \text{ g}$$

which is the deficient mass quoted in the report.

TABLE 2

PREVIOUS GRAVITY SURVEYS

REFERENCE	YEAR OF SURVEY	AREA	RESULTS OF SIGNIFICANCE TO 1974 GRAVITY WORK
Langron (1956)	1954	Embayment	Variable densities within sediments. Complexity of area. Density information.
Stott & Langron (1959)	1955-1957	Darwin-Katherine area	Gravity lows over granites in the Darwin-Katherine area. Density information.
Daly & Tate (1960)	1957	Waterhouse No. 2	Gravity low associated with Waterhouse Complex. Gradient near Complex approx 3.5 milligal/km.
Daly, Horvath & Tate (1962)	1957	Embayment	Variable density within sediments. Complexity of area. Browns orebody too small to give recognisable anomaly.
Duckworth, Farrow & Gardener (1968)	1966	Rum Jungle East and Woodcutters L5	Detailed survey over mineralisation at 100 m depth. Reconnaissance traverses showed gravity decreasing toward Rum Jungle Complex with gradient approximately 4.7 milligal/km.
Williams (1970)	1967	Eastern margin of Rum Jungle Complex	Gravity low on Rum Jungle Complex. Large body of non-magnetic amphibolite. Gravity lows on Coomalie and Celia Dolomites. Density information.

TABLE 2 (Continued)

REFERENCE	YEAR OF SURVEY	AREA	RESULTS OF SIGNIFICANCE TO 1974 GRAVITY WORK
Whitworth (1970)	1967	Parts of the Northern Territory and Western Australia	Shows that 1974 survey area lies near the boundary between the Tipperary Regional Gravity Low and the Marrakai Gravity Plateau.
Gardener (1971)	1968	EW traverse across Rum Jungle Complex on line 120S of the Rum Jungle East grid	Dip of boundary between Complex and metasediments was 70^{o} on western margin of the Complex. Density contrast 0.13 g/cm^{-3}.

PLATE I

North Australian Railway

FAULT

HIGHWAY

REEF

EMBAYMENT AREA

Manton Dam

Batchelor

Adelaide River

GIANTS

STUART

KILOMETRES 0 5

REFERENCE

UPPER PROTEROZOIC

Tolmer Group

Puo — Buldiva Sandstone; Depot Creek Sandstone Member

LOWER PROTEROZOIC

Finniss River Group

Plb — Burrell Creek Formation: Quartz greywacke, Lithic greywacke

Amphibolite

Goodparla Group

Pld — Golden Dyke Formation

Masson Formation

Pla — Acacia Gap Tongue

Batchelor Group

Plo — Coomalie Dolomite

Plr — Crater Formation: Quartz pebble conglomerate; Quartz hematite boulder conglomerate

Pll — Celia Dolomite

Ple — Beestons Formation

ARCHAEAN–?MIDDLE PROTEROZOIC

A-Pgt — Waterhouse Complex

A-Pgr — Rum Jungle Complex

Geological boundary

Anticline showing plunge

Syncline showing plunge

Fault

Strike and dip of beds

Vertical beds

Overturned beds

Trend of bedding, showing direction of dip

Direction of plunge

Solid geology map of the Rum Jungle area. Record No. 1977/9

D52/B7-651

PLOTTED 24/06/75

RUM JUNGLE
NORTHERN TERRITORY

PLATE 2
UNITS
HEIGHT : METRES
GRAVITY : MILLIGALS

AUSTRALIA 1 / 50000.

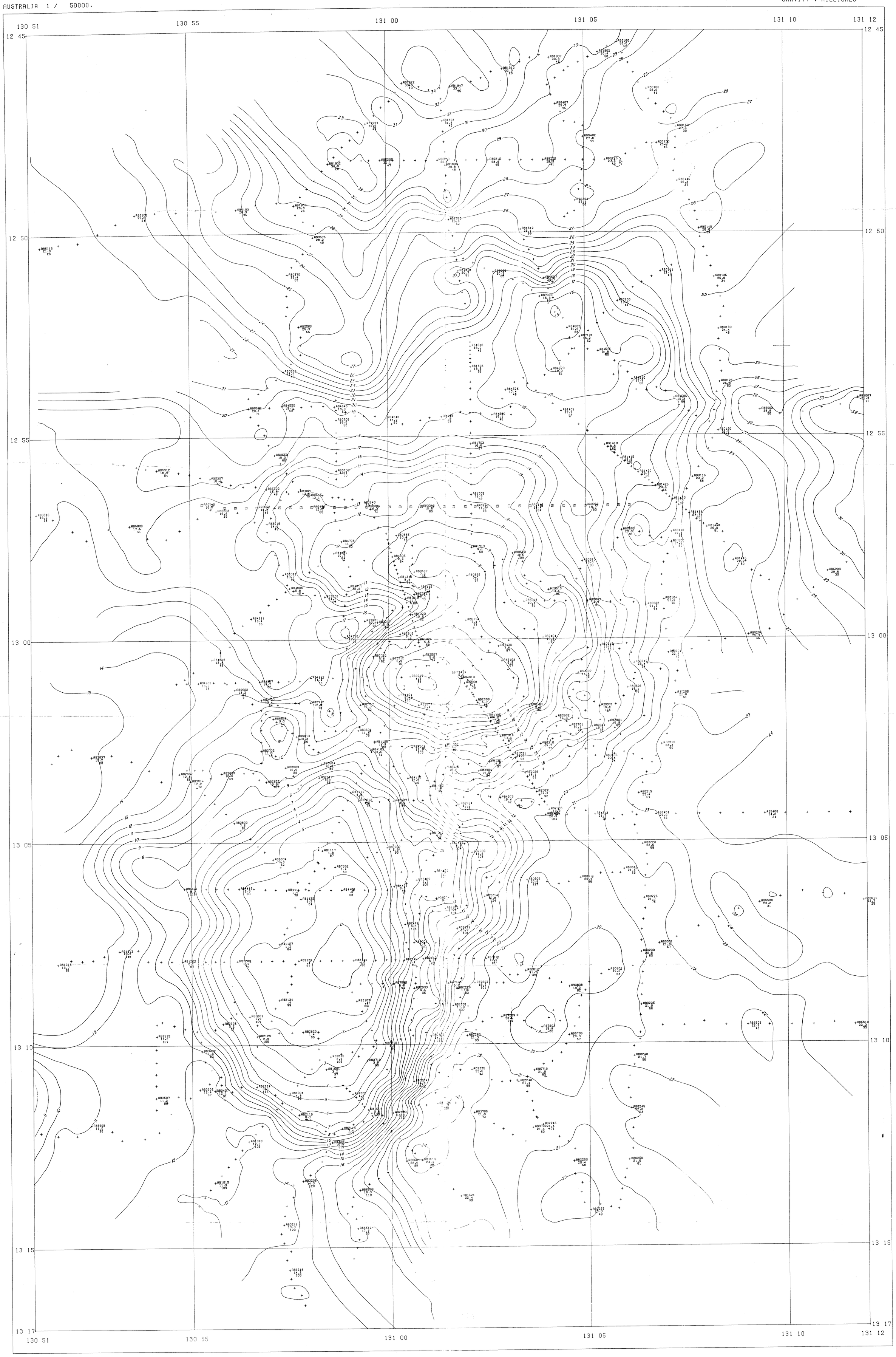

CLARKE 1858 SPHEROID
TRANSVERSE MERCATOR PROJECTION
ZONE 4 (AUSTRALIA SERIES)

⊡ AA = 6819
\+ AB = 7408

BOUGUER ANOMALIES
(REGIONAL GRADIENT INCLUDED)

DENSITY = 2.67 GMS/CC.

LEGEND

A1234 ; STATION NUMBER
56.7 ; GRAVITY ANOMALY
456 ; GROUND ELEVATION

RUM JUNGLE
NORTHERN TERRITORY

D52/B2-4+8

CONTOUR LEVELS AT
1.00 AND 10.00 **D52/B7-654**

Record No. 1977/9

PLOTTED 17/07/75

RUM JUNGLE
NORTHERN TERRITORY

AUSTRALIA 1 / 50000.

PLATE 3
UNITS
HEIGHT ; METRES
GRAVITY ; MILLIGALS

130 51 · 130 55 · 131 00 · 131 05 · 131 10 · 131 12
12 45 · 12 50 · 12 55 · 13 00 · 13 05 · 13 10 · 13 15 · 13 17

CLARKE 1858 SPHEROID
TRANSVERSE MERCATOR PROJECTION
ZONE 4 (AUSTRALIA SERIES)

□ AA = 6819
+ AB = 7408

BOUGUER ANOMALIES
(REGIONAL GRADIENT REMOVED)

DENSITY = 2.67 GMS/CC.

LEGEND

A1234 ; STATION NUMBER
56.7 ; GRAVITY ANOMALY
456 ; GROUND ELEVATION

RUM JUNGLE
NORTHERN TERRITORY

D52/B2-4+8

CONTOUR LEVELS AT
1.00 AND 10.00

Record No.1977/9

D52/B7-655

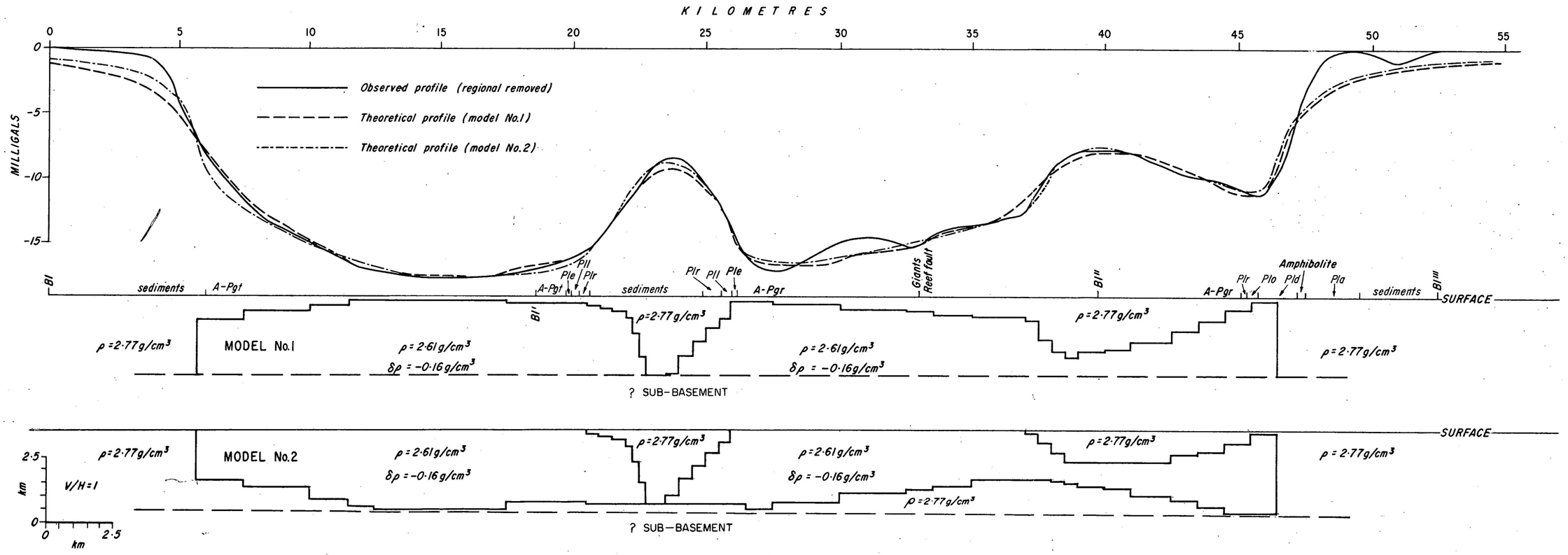

PROFILE BI–BI'–BI''–BI'''
RUM JUNGLE AND WATERHOUSE COMPLEXES

Record No. 1977/9

D52/B7-660

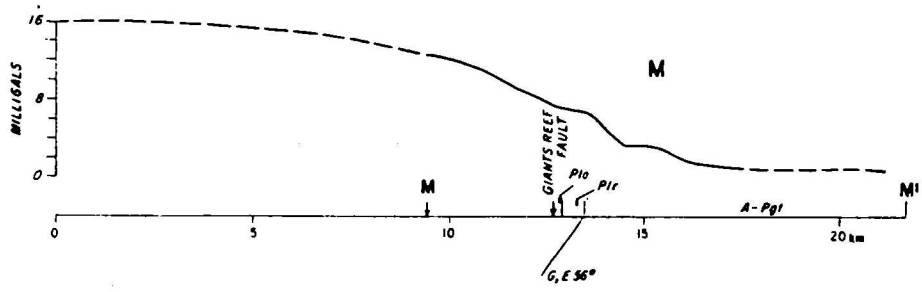

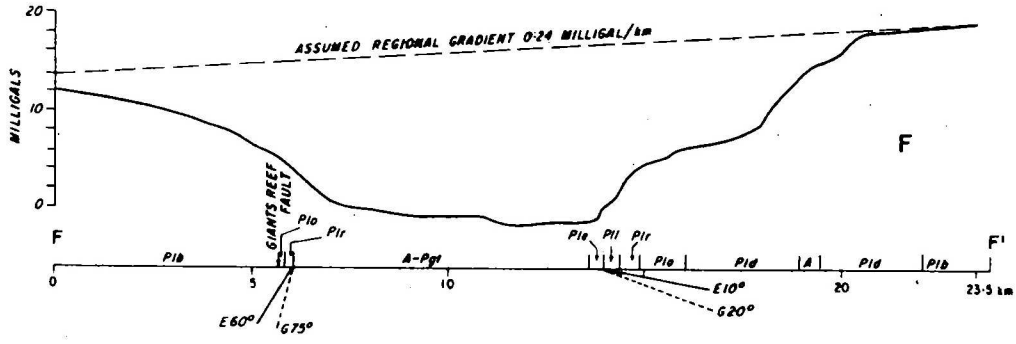

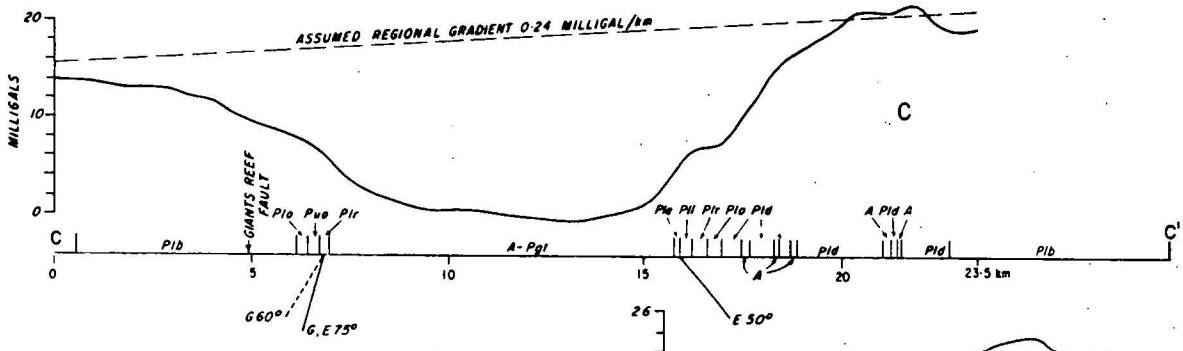

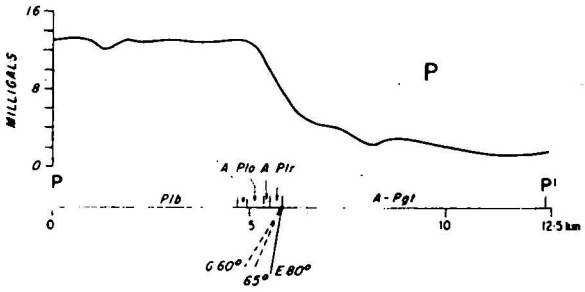

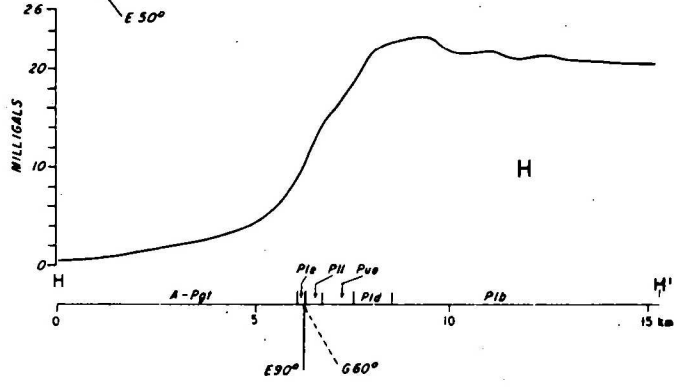

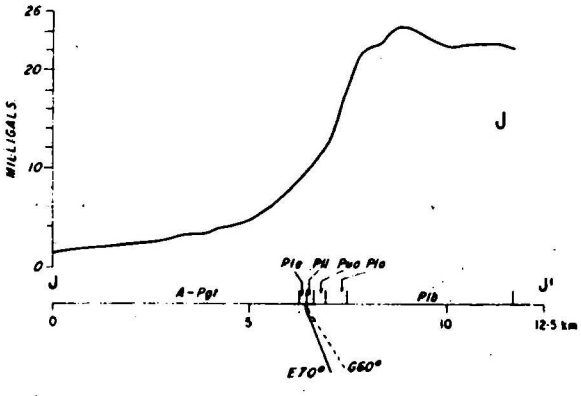

E From gravity data

G From geological data

DIP ESTIMATES AROUND THE WATERHOUSE COMPLEX